



ELSEVIER

Available online at www.sciencedirect.com

SCIENCE @ DIRECT®

Palaeogeography, Palaeoclimatology, Palaeoecology 222 (2005) 53–76

PALAEO

www.elsevier.com/locate/palaeo

Upper Ordovician (Mohawkian) carbon isotope ($\delta^{13}\text{C}$) stratigraphy in eastern and central North America: Regional expression of a perturbation of the global carbon cycle

Seth A. Young*, Matthew R. Saltzman, Stig M. Bergström

Department of Geological Sciences, The Ohio State University, 275 Mendenhall Laboratory, 125 S. Oval Mall, Columbus, OH 43210, USA

Received 2 September 2004; received in revised form 10 March 2005; accepted 10 March 2005

Abstract

The Guttenberg carbon isotope excursion (GICE) documented from eastern North America demonstrates the effects that regional, geochemically distinct water masses, upwelling, and ocean circulation have on the carbon isotope record from carbonate platforms. Late Turinian–Chatfieldian carbonates from Oklahoma, Kentucky, Virginia, and West Virginia record a positive carbon isotope excursion ($\geq +3.0\text{‰}$), the GICE excursion. The GICE excursion has relations to established biostratigraphy (beginning in the North American Midcontinent *Phragmodus undatus* Conodont Zone and continuing through the *Plectodina tenuis* Zone), sequence, and event stratigraphy. Previously established models for positive carbon isotope shifts on carbonate platforms have been tested during the GICE excursion, where geochemically distinct water masses are defined for the Upper Ordovician. A major eustatic sea-level rise before the GICE promoted a greater exchange of open ocean waters onto the carbonate platform of Laurentia; however, restricted or sluggish circulation and exchange between water masses within the epeiric seas and the adjacent Iapetus Ocean were still apparent. Local variations documented in the GICE excursion are directly related to upwelling of nutrient rich isotopically light waters, increased primary productivity, and the subsequent organic carbon production and burial.

© 2005 Published by Elsevier B.V.

Keywords: Late Ordovician; Carbon isotope; Water masses; Upwelling; Carbonate platform

1. Introduction

The Late Ordovician (Mohawkian) epeiric sea of eastern North America has been divided into

temperature–salinity-defined water masses based upon regional variations in faunal patterns and carbon and neodymium isotopes in marine carbonates (Holmden et al., 1998). These proposed geochemically distinct water masses are referred to as “aquafacies” because they are reflected in both faunas and lithologies of the underlying sedimentary deposits. Recognition of these aquafacies across the

* Corresponding author.

E-mail address: young.899@osu.edu (S.A. Young).

Mohawkian carbonate platform potentially indicates sluggish or restricted circulation within epeiric seas and between epeiric seas and adjacent oceans (Holmden et al., 1998). However, this model has only been rigorously examined for a brief time slice of $\sim 10^5$ years defined by two prominent K-bentonite horizons (“Deicke–Millbrig time slice”). Much less is known about how the epeiric sea aquafacies patterns varied through time ($>10^5$ years), particularly in association with oceanographic events such as a carbon isotope excursion (e.g., Patzkowsky et al., 1997). This is important because local water mass differences in $\delta^{13}\text{C}$ can provide information regarding nutrient cycling, which influences the strength of the biological pump, atmospheric CO_2 levels, and global climate (e.g., Sigman and Boyle, 2000).

The shallow epeiric seas that covered most of eastern and central North America during the Late Ordovician record a significant positive carbon isotope excursion of $\sim +3\%$ (Hatch et al., 1987; Ludvigson et al., 1996; Patzkowsky et al., 1997; Simo et al., 2003). This excursion was first documented in organic matter from the Guttenberg Limestone Member of the Decorah Formation in the Upper Mississippi Valley (Hatch et al., 1987) and is here referred to as the Guttenberg carbon isotope excursion (GICE). The GICE has since been documented at many sections in the Mohawkian (Chatfieldian Stage) Guttenberg Limestone Member of the Decorah Formation in the Upper Mississippi Valley (Ludvigson et al., 1996, 2000, 2004) and in the Salona Formation of Pennsylvania (Patzkowsky et al., 1997) as well as time equivalent carbonates worldwide (Ainsaar et al., 1999). The correlation of the GICE worldwide is facilitated by its occurrence above several widespread K-bentonite horizons deposited during extensive explosive volcanism associated with the Taconic Orogeny (Kolata et al., 1996; Simo et al., 2003). Apart from the well known Hirnantian (latest Ordovician) positive excursion, which is associated with widespread glaciation and mass extinction (Brenchley et al., 1994, 2003), the GICE is the most significant $\delta^{13}\text{C}$ excursion documented in the Ordovician.

While the GICE is known to coincide with biotic and paleoceanographic changes that in North America

led to a fundamental shift in the style of platform sedimentation from tropical-type to temperate-type carbonates with associated chert and phosphate (Holmden and Patzkowsky, 1996; Kolata et al., 2001; Pope and Steffen, 2003), the cause(s) of the inferred high organic carbon burial remain uncertain. Patzkowsky et al. (1997) suggested that a relative deepening in the Taconic foreland basin (Taconic “aquafacies”) of eastern Laurentia, led to enhanced burial of isotopically light (^{13}C -depleted) organic matter in poorly oxygenated deep water masses. Increased nutrient fluxes from the Taconic highlands may have contributed to locally high organic carbon burial by stimulating surface ocean production (Holmden et al., 1998).

A role for upwelling as a source of increased nutrients to the Taconic aquafacies has also been considered. However, because the observed offset of $\sim 2.0\%$ in $\delta^{13}\text{C}_{\text{carb}}$ values between the isotopically light Midcontinent water mass (affected by upwelling) and the heavier Taconic aquafacies remained constant before and during the GICE, this suggests that the intensity of upwelling changed little during the Middle to Late Ordovician (Patzkowsky et al., 1997; Holmden et al., 1998). The importance of the onset of vigorous upwelling in platform margin settings such as Oklahoma (e.g. Pope and Steffen, 2003) has not been examined as a source of nutrients and enhanced productivity that influenced regional and global $\delta^{13}\text{C}_{\text{carb}}$ values during the Chatfieldian. Examining the evidence for upwelling and $\delta^{13}\text{C}$ values in platform margin settings (e.g. Oklahoma) could document any potential relation of upwelling to the GICE.

The purpose of this paper is to integrate high resolution carbon isotope ($\delta^{13}\text{C}$) data from several Late Ordovician (Chatfieldian Stage) carbonate sections from widely separated basins across eastern Laurentia as well as a platform margin section in Oklahoma. These data are then used to establish relations of this positive $\delta^{13}\text{C}$ excursion ($\sim +3.0\%$) to previously established aquafacies and changing paleoceanography during the Late Ordovician. Carbon isotope data from these sections are correlated across North America based upon relations of the GICE to the established Ordovician biostratigraphy, sequence and K-bentonite event stratigraphy.

2. Geologic background

Most of eastern and central North America during the Late Ordovician was situated between 15° and 30° S (Fig. 1). Four sections in this region are particularly suitable for comparison with previously published $\delta^{13}\text{C}$ data from the Midcontinent and Taconic Foreland Basin of North America. The sections include (1) the Bromide and Viola Springs Formations in the Arbuckle Mountains of south-central Oklahoma (Alberstadt, 1973; Sweet, 1983); (2) the Eggleston and Trenton Limestones in southwestern Virginia (Fetzer, 1973; Hall, 1986; Leslie, 1995); (3) the Tyrone and Lexington Limestones of north-central Kentucky (Sweet et al., 1974; Sweet, 1979); and (4) the Nealmont and Dolly Ridge Formations in West Virginia (Perry, 1972; Keith and Hall, 1989; Keith, 1989). These sections were chosen because they represent thick carbonate sequences, where biostratigraphy (conodonts and/or graptolites), sequence stratigraphy and/or K-bentonite event stratigraphy have been previously investigated. Coupling biostratigraphic, sequence and event stratigraphic data, with chemostratigraphic data allows for a unique view into Earth's history during this particular perturbation of the global carbon cycle.

2.1. Conodont and graptolite biostratigraphy

Conodont biostratigraphy is well established (Sweet, 1984a; Hall, 1986; Haynes, 1994; Leslie, 1995; Richardson and Bergström, 2003) for the study interval in the Upper Ordovician in North America. In the Mohawkian there are six conodont zones in the Midcontinent of North America, in ascending order, the *Plectodina aculeata*, *Erismodus quadridactylus*, *Phragmodus undatus*, *Plectodina tenuis*, and *Belodina confluens* Zones. Although first defined by graphic correlation techniques (Sweet, 1984a), for practical purposes these zones have been recognized by the first appearance of the zonal index species. The GICE begins near the top of the *P. undatus* Zone and ends within the *P. tenuis* Zone.

Graptolite biostratigraphy is established for the Middle and Upper Ordovician in North America. In the North American Middle Ordovician, there are six graptolite zones, in stratigraphic order; the *Nema-graptus gracilis*, *Climacograptus bicornis*, *Climacograptus americanus*, *Orthograptus ruedemanni*, and *Climacograptus spiniferus* Zones. Previously, the $\delta^{13}\text{C}$ excursion had not been documented from sections containing good graptolite biostratigraphy, but it could be inferred to occur within the *C. americanus* Zone. The Fittstown, Oklahoma section,

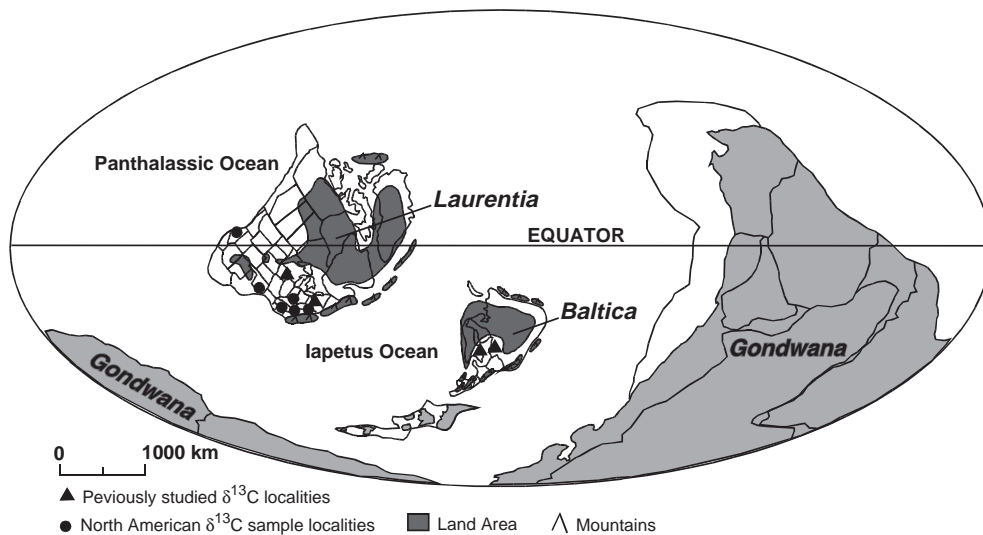


Fig. 1. Late Middle Ordovician paleogeographic reconstruction (modified from Witzke, 1990; Scotese and McKerrow, 1991) showing positions of sections in Oklahoma, Kentucky, Virginia, and West Virginia, along with previously studied sections in Baltica and Laurentia (Ludvigson et al., 1996; Patzkowsky et al., 1997; Ainsaar et al., 1999).

described in this study, offers one of the thickest and most complete sections of Chatfieldian carbonates in the Arkhoma Basin, where a good graptolite and conodont biostratigraphy is available. The $\delta^{13}\text{C}$ excursion occurs above the *C. bicornis* Zone and below the first appearance of the graptolite *C. spiniferus*, thus placing the excursion within the *C. americanus* and *O. ruedemanni* Zones (Saltzman et al., 2003).

2.2. Sequence and K-bentonite event stratigraphy

Ordovician K-bentonites constitute nearly isochronous rock units useful in precise correlations and are applicable to biogeographic, paleogeographic, paleoecologic, and sedimentologic investigations on both local and regional scales (Kolata et al., 1996; Simo et al., 2003). A chemical fingerprinting technique, based on the relative proportions of rare earth elements present in the altered volcanic ash beds, has been used to correlate K-bentonites across eastern North America. A section at Hagan, Virginia, described in this study, offers one of the thickest and most complete sequences of Turinian through Chatfieldian carbonates from the Taconic foreland basin, and contains the Hockett, Ocoonita, Deicke, Millbrig, V-7, and “House Springs” K-bentonites (Kolata et al., 1998). The $\delta^{13}\text{C}$ excursion begins anywhere from 3–5 m

above the Millbrig K-bentonite bed in North America. The Millbrig K-bentonite is correlated with the Kinnekulle K-bentonite in Baltoscandia based on biostratigraphic and geochemical data (Huff et al., 1992; Bergström et al., 1995, 2004; Saltzman et al., 2003), and the GICE also occurs ~3–8 m above the Kinnekulle K-bentonite in Baltoscandian sections.

A sequence stratigraphic framework for the Middle and Upper Ordovician has been defined by Holland and Patzkowsky (1996), in which they recognized six depositional sequences in the Mohawkian (M1 through M6). Holland and Patzkowsky (1996) also recognized a major sea level rise (“Trenton Transgression”) across the M4–M5 sequence boundary, during which carbonates shift from a tropical-type to a temperate-type. Tropical-type carbonates prior to the M5 sequence display a wide variety of carbonate lithofacies ranging from skeletal carbonates to lime mudstones, but the dominant lithofacies were fine-grained. Above the M5 sequence boundary, a more limited variety of temperate-type carbonates were deposited, composed of skeletal grainstones and packstones, with widespread phosphatization. Patzkowsky et al. (1997) suggested that the GICE in Pennsylvania coincides with the M4–M5 sequence boundary which indicates that sea-level rise and oceanographic changes are associated with major perturbations of the carbon cycle.

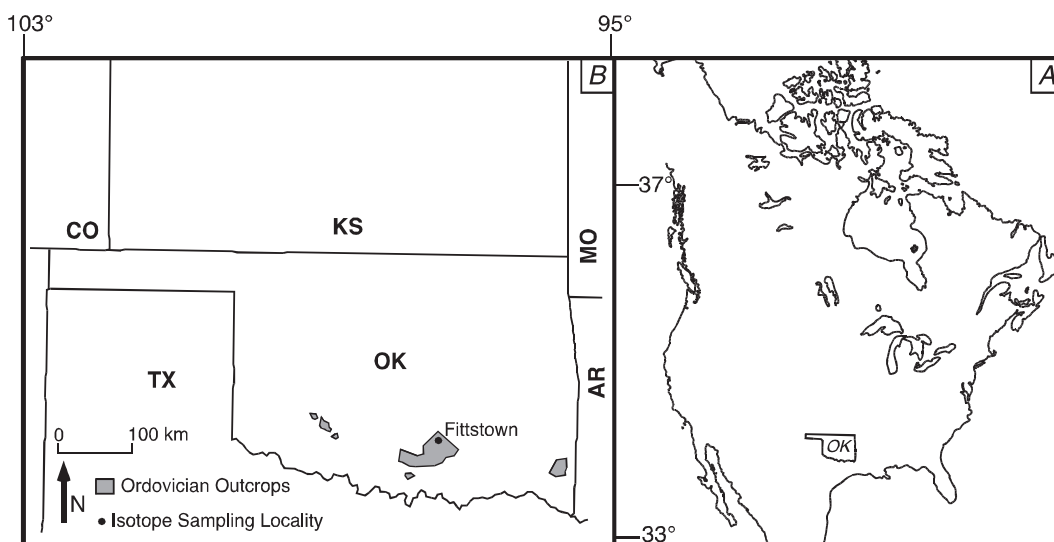


Fig. 2. (A) Map of North America showing an outline of Oklahoma (OK). (B) Locality map showing Ordovician outcrops in Oklahoma and the position of the isotope sampling locality near Fittstown.

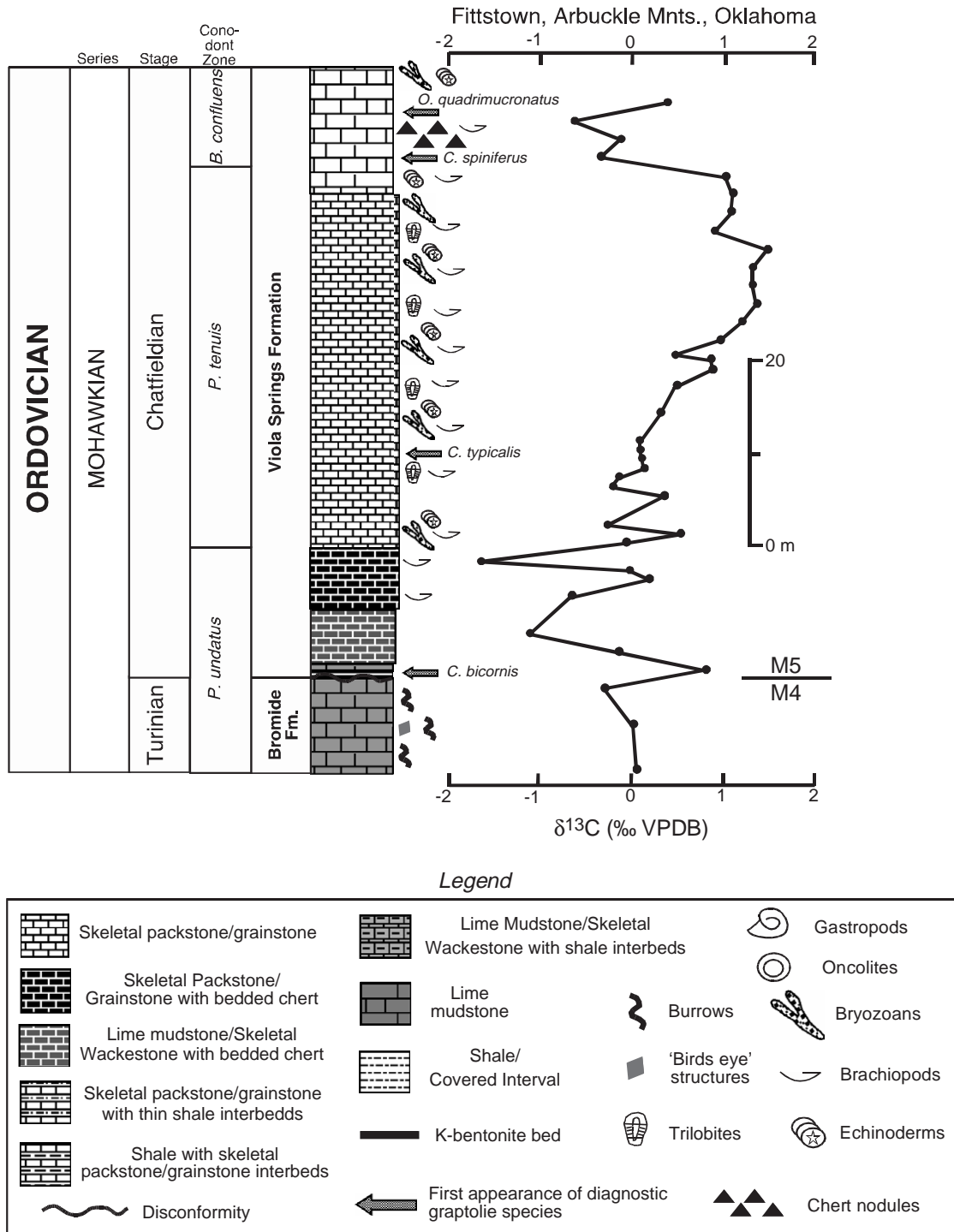


Fig. 3. Stratigraphic column, lithologic legend, and $\delta^{13}\text{C}$ plots from the Fittstown section, Arbuckle Mountains, Oklahoma. Conodont zonation based on Sweet (1983) and graptolite occurrences based on Finney (1986).

3. Methods

In this paper, high-resolution $\delta^{13}\text{C}$ curves were constructed from 296 samples run from the upper part of the *P. undatus* Zone through the lower part of the *B. confluens* Zone (late Turinian–Chatfieldian Stages). $\delta^{13}\text{C}$ curves have been generated from a range of carbonate (fine to coarse-grained) lithologies collected from four sections in eastern and central North America where conodont biostratigraphy and/or K-

bentonite event stratigraphy have previously been established. Micritic components were preferentially sampled by using a drill assembly on polished thin-section billets. In samples where micritic components were limited, a portion of the sample that was representative of the entire carbonate sample was drilled.

Carbonate powders from this study were analyzed at labs at the University of Michigan, Texas A and M University, and University of Saskatch-

Table 1
Stable isotope data, Fittstown, Oklahoma

Meters*	$\delta^{13}\text{C}$	$\delta^{18}\text{O}$	Conodont zone	Stage	Formation	Lithology
0.0	0.06	−4.41	<i>undatus</i>	Turinian	Bromide	lime mudstone
5.0	0.02	−3.68	<i>undatus</i>	Turinian	Bromide	lime mudstone
9.0	−0.28	−3.35	<i>undatus</i>	Turinian	Bromide	lime mudstone
11.0	0.81	−4.13	<i>undatus</i>	Chatfieldian	Viola Springs	lime mudstone
13.0	−0.15	−4.69	<i>undatus</i>	Chatfieldian	Viola Springs	wackestone/bedded chert
15.0	−1.11	−4.84	<i>undatus</i>	Chatfieldian	Viola Springs	wackestone/bedded chert
19.0	−0.66	−4.21	<i>undatus</i>	Chatfieldian	Viola Springs	packstone/bedded chert
21.0	0.20	−4.10	<i>undatus</i>	Chatfieldian	Viola Springs	packstone/bedded chert
22.0	−0.01	−4.37	<i>undatus</i>	Chatfieldian	Viola Springs	packstone/bedded chert
23.0	−1.64	−4.73	<i>undatus</i>	Chatfieldian	Viola Springs	grainstone/bedded chert
25.0	−0.06	−4.85	<i>undatus</i>	Chatfieldian	Viola Springs	skeletal grainstone
26.0	0.54	−4.45	<i>tenuis</i>	Chatfieldian	Viola Springs	skeletal grainstone
27.0	−0.25	−4.74	<i>tenuis</i>	Chatfieldian	Viola Springs	skeletal grainstone
30.0	0.36	−4.65	<i>tenuis</i>	Chatfieldian	Viola Springs	skeletal grainstone
31.0	−0.21	−4.58	<i>tenuis</i>	Chatfieldian	Viola Springs	skeletal grainstone
32.0	−0.13	−4.51	<i>tenuis</i>	Chatfieldian	Viola Springs	skeletal grainstone
33.0	0.15	−4.94	<i>tenuis</i>	Chatfieldian	Viola Springs	skeletal grainstone
34.0	0.13	−5.18	<i>tenuis</i>	Chatfieldian	Viola Springs	skeletal grainstone
35.0	0.11	−4.37	<i>tenuis</i>	Chatfieldian	Viola Springs	skeletal grainstone
36.0	0.10	−4.82	<i>tenuis</i>	Chatfieldian	Viola Springs	skeletal grainstone
39.0	0.32	−4.63	<i>tenuis</i>	Chatfieldian	Viola Springs	skeletal grainstone
42.0	0.49	−4.81	<i>tenuis</i>	Chatfieldian	Viola Springs	skeletal grainstone
44.0	0.91	−5.01	<i>tenuis</i>	Chatfieldian	Viola Springs	skeletal grainstone
45.0	0.87	−4.89	<i>tenuis</i>	Chatfieldian	Viola Springs	skeletal grainstone
45.5	0.48	−5.01	<i>tenuis</i>	Chatfieldian	Viola Springs	skeletal packstone
47.0	0.97	−4.36	<i>tenuis</i>	Chatfieldian	Viola Springs	skeletal packstone
49.0	1.22	−4.38	<i>tenuis</i>	Chatfieldian	Viola Springs	skeletal packstone
51.0	1.38	−4.60	<i>tenuis</i>	Chatfieldian	Viola Springs	skeletal packstone
53.0	1.33	−4.80	<i>tenuis</i>	Chatfieldian	Viola Springs	skeletal packstone
55.0	1.34	−4.71	<i>tenuis</i>	Chatfieldian	Viola Springs	skeletal packstone
57.0	1.49	−4.04	<i>tenuis</i>	Chatfieldian	Viola Springs	skeletal packstone
59.0	0.93	−4.79	<i>tenuis</i>	Chatfieldian	Viola Springs	skeletal packstone
61.0	1.09	−4.55	<i>tenuis</i>	Chatfieldian	Viola Springs	skeletal packstone
63.0	1.11	−4.71	<i>tenuis</i>	Chatfieldian	Viola Springs	lime mudstone
65.0	1.04	−4.33	<i>tenuis</i>	Chatfieldian	Viola Springs	wackestone/ bedded chert
67.0	−0.33	−5.27	<i>tenuis</i>	Chatfieldian	Viola Springs	wackestone/ bedded chert
69.0	−0.12	−4.75	<i>tenuis</i>	Chatfieldian	Viola Springs	lime mudstone
71.0	−0.62	−5.00	<i>tenuis</i>	Chatfieldian	Viola Springs	skeletal wackestone
73.0	0.38	−4.62	<i>tenuis</i>	Chatfieldian	Viola Springs	skeletal wackestone

* Section begins 10 m below the Viola Springs/Bromide Contact, which is sharp and an unconformable contact.

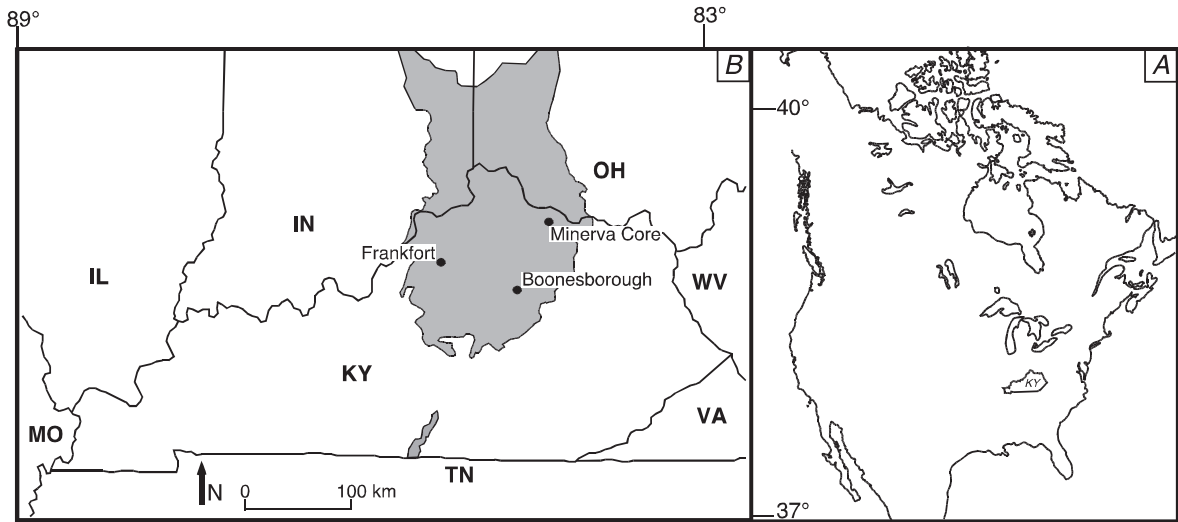


Fig. 4. (A) Map of North America showing an outline of Kentucky (KY). (B) Locality map showing Ordovician outcrops in the Cincinnati Arch region of Kentucky, Indiana, and Ohio and carbon isotope sampling localities at Boonesborough, Frankfort, and the Minerva drill core site.

ewan. Carbonate samples were heated for 1 h at 380 °C and then reacted with 100% H₃PO₄ at 72 °C in a Finnigan Kiel extraction system coupled directly to a Finnigan mass spectrometer. All isotope ratios are reported in per mil relative to the VPDB standard.

Carbonate rocks are rarely homogeneous and are more commonly mixtures of skeletal (i.e. brachiopods, bryozoans, trilobites, echinoderms) and non-skeletal grains (i.e. ooids, pellets, intraclasts). Calcite from brachiopods is considered by some (Marshall et al., 1997; Azmy et al., 1998; Mii et al., 1999) to be the

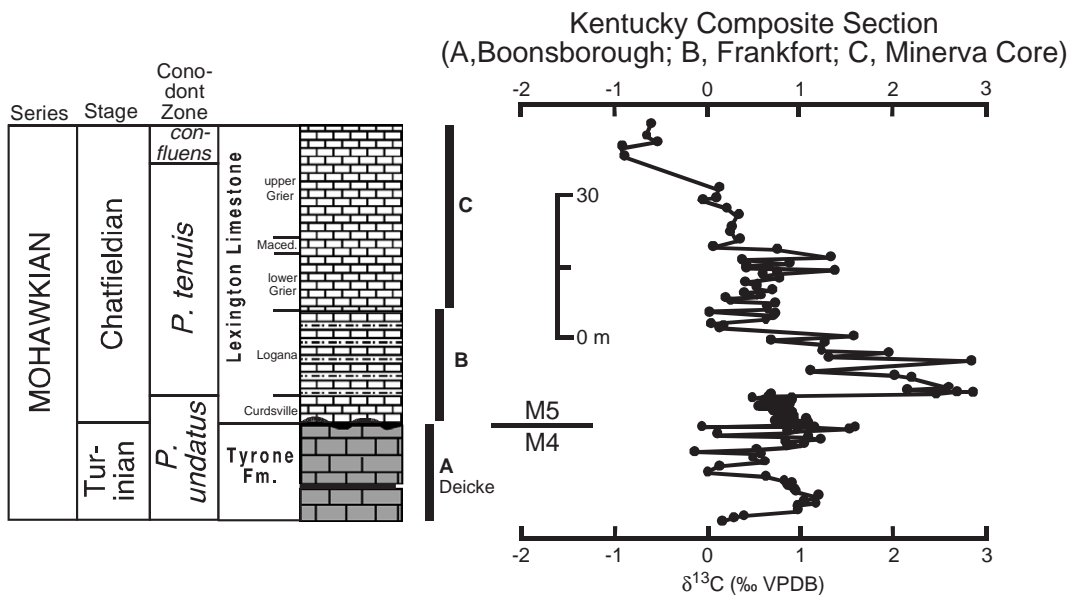


Fig. 5. A composite plot of δ¹³C of carbonates from Boonesborough, Frankfort, and the Minerva core in Kentucky. Conodont zonation based on Votaw (1971), Sweet et al. (1974), and Sweet (1979).

Table 2

Stable isotope data, Kentucky composite section (Frankfort, Boonsborough, Minerva core)

Meters	$\delta^{13}\text{C}$	$\delta^{18}\text{O}$	Conodont zone	Stage	Formation	Section
0	0.16	-3.70	<i>undatus</i>	Turinian	Tyrone	Boonsborough
0.5	0.28	-4.46	<i>undatus</i>	Turinian	Tyrone	Boonsborough
1	0.37	-4.87	<i>undatus</i>	Turinian	Tyrone	Boonsborough
2	0.96	-5.09	<i>undatus</i>	Turinian	Tyrone	Boonsborough
3	0.96	-5.22	<i>undatus</i>	Turinian	Tyrone	Boonsborough
3.5	1.15	-4.08	<i>undatus</i>	Turinian	Tyrone	Boonsborough
4	1.02	-4.04	<i>undatus</i>	Turinian	Tyrone	Boonsborough
5	1.19	-3.49	<i>undatus</i>	Turinian	Tyrone	Boonsborough
6	0.93	-4.02	<i>undatus</i>	Turinian	Tyrone	Boonsborough
6.5	0.92	-5.23	<i>undatus</i>	Turinian	Tyrone	Boonsborough
7	0.85	-4.82	<i>undatus</i>	Turinian	Tyrone	Boonsborough
7.5	0.90	-4.83	<i>undatus</i>	Turinian	Tyrone	Boonsborough
8	0.82	-4.39	<i>undatus</i>	Turinian	Tyrone	Boonsborough
9	0.63	-5.60	<i>undatus</i>	Turinian	Tyrone	Boonsborough
10	0.00	-5.45	<i>undatus</i>	Turinian	Tyrone	Boonsborough
11	0.12	-5.06	<i>undatus</i>	Turinian	Tyrone	Boonsborough
12	0.60	-5.76	<i>undatus</i>	Turinian	Tyrone	Boonsborough
13	0.51	-4.53	<i>undatus</i>	Turinian	Tyrone	Boonsborough
13.5	0.55	-5.81	<i>undatus</i>	Turinian	Tyrone	Boonsborough
14	-0.15	-4.63	<i>undatus</i>	Turinian	Tyrone	Boonsborough
14.5	0.51	-4.42	<i>undatus</i>	Turinian	Tyrone	Boonsborough
15	0.86	-4.36	<i>undatus</i>	Turinian	Tyrone	Boonsborough
15.5	1.02	-5.12	<i>undatus</i>	Turinian	Tyrone	Frankfort
16	0.83	-4.57	<i>undatus</i>	Turinian	Tyrone	Frankfort
16.5	1.20	-4.36	<i>undatus</i>	Turinian	Tyrone	Frankfort
17	1.08	-4.31	<i>undatus</i>	Turinian	Tyrone	Frankfort
17.5	0.10	-5.17	<i>undatus</i>	Turinian	Tyrone	Frankfort
18	0.86	-5.28	<i>undatus</i>	Turinian	Tyrone	Frankfort
18.25	0.96	-4.64	<i>undatus</i>	Turinian	Tyrone	Frankfort
18.5	1.51	-4.19	<i>undatus</i>	Turinian	Tyrone	Frankfort
18.75	1.57	-3.98	<i>undatus</i>	Turinian	Tyrone	Frankfort
19	1.13	-4.74	<i>undatus</i>	Turinian	Tyrone	Frankfort
19.25	-0.05	-4.98	<i>undatus</i>	Chatfieldian	Lexington Limestone	Frankfort
19.5	0.88	-5.03	<i>undatus</i>	Chatfieldian	Lexington Limestone	Frankfort
19.75	1.08	-4.54	<i>undatus</i>	Chatfieldian	Lexington Limestone	Frankfort
20	0.72	-5.33	<i>undatus</i>	Chatfieldian	Lexington Limestone	Frankfort
20.25	0.91	-5.46	<i>undatus</i>	Chatfieldian	Lexington Limestone	Frankfort
20.5	1.06	-5.40	<i>undatus</i>	Chatfieldian	Lexington Limestone	Frankfort
20.75	0.74	-6.08	<i>undatus</i>	Chatfieldian	Lexington Limestone	Frankfort
21	0.93	-5.39	<i>undatus</i>	Chatfieldian	Lexington Limestone	Frankfort
21.25	0.81	-5.42	<i>undatus</i>	Chatfieldian	Lexington Limestone	Frankfort
21.5	0.88	-5.72	<i>undatus</i>	Chatfieldian	Lexington Limestone	Frankfort
21.75	0.90	-4.93	<i>undatus</i>	Chatfieldian	Lexington Limestone	Frankfort
22	0.90	-5.35	<i>undatus</i>	Chatfieldian	Lexington Limestone	Frankfort
22.25	0.70	-5.74	<i>undatus</i>	Chatfieldian	Lexington Limestone	Frankfort
22.5	0.80	-4.82	<i>undatus</i>	Chatfieldian	Lexington Limestone	Frankfort
22.75	0.83	-4.79	<i>undatus</i>	Chatfieldian	Lexington Limestone	Frankfort
23	0.58	-5.41	<i>undatus</i>	Chatfieldian	Lexington Limestone	Frankfort
23.25	0.54	-5.42	<i>undatus</i>	Chatfieldian	Lexington Limestone	Frankfort
23.5	0.88	-4.87	<i>undatus</i>	Chatfieldian	Lexington Limestone	Frankfort
23.75	0.65	-5.46	<i>undatus</i>	Chatfieldian	Lexington Limestone	Frankfort
24	0.63	-5.71	<i>undatus</i>	Chatfieldian	Lexington Limestone	Frankfort
24.25	0.90	-4.40	<i>undatus</i>	Chatfieldian	Lexington Limestone	Frankfort

Table 2 (continued)

Meters	$\delta^{13}\text{C}$	$\delta^{18}\text{O}$	Conodont zone	Stage	Formation	Section
24.5	0.60	-5.83	<i>undatus</i>	Chatfieldian	Lexington Limestone	Frankfort
24.75	0.90	-5.07	<i>undatus</i>	Chatfieldian	Lexington Limestone	Frankfort
25	0.51	-5.47	<i>tenuis</i>	Chatfieldian	Lexington Limestone	Frankfort
25.25	0.65	-6.12	<i>tenuis</i>	Chatfieldian	Lexington Limestone	Frankfort
25.5	0.67	-5.52	<i>tenuis</i>	Chatfieldian	Lexington Limestone	Frankfort
25.75	2.45	-5.42	<i>tenuis</i>	Chatfieldian	Lexington Limestone	Frankfort
26	2.67	-4.27	<i>tenuis</i>	Chatfieldian	Lexington Limestone	Frankfort
26.25	2.84	-4.81	<i>tenuis</i>	Chatfieldian	Lexington Limestone	Frankfort
26.5	2.13	-4.84	<i>tenuis</i>	Chatfieldian	Lexington Limestone	Frankfort
27	2.58	-4.91	<i>tenuis</i>	Chatfieldian	Lexington Limestone	Frankfort
29	2.18	-4.87	<i>tenuis</i>	Chatfieldian	Lexington Limestone	Frankfort
29.5	2.01	-5.06	<i>tenuis</i>	Chatfieldian	Lexington Limestone	Frankfort
30.5	1.12	-5.23	<i>tenuis</i>	Chatfieldian	Lexington Limestone	Frankfort
32.5	2.82	-4.76	<i>tenuis</i>	Chatfieldian	Lexington Limestone	Frankfort
33.5	1.31	-5.14	<i>tenuis</i>	Chatfieldian	Lexington Limestone	Frankfort
34	1.93	-6.08	<i>tenuis</i>	Chatfieldian	Lexington Limestone	Frankfort
34.5	1.21	-5.42	<i>tenuis</i>	Chatfieldian	Lexington Limestone	Frankfort
36	1.25	-5.80	<i>tenuis</i>	Chatfieldian	Lexington Limestone	Frankfort
36.5	0.68	-5.90	<i>tenuis</i>	Chatfieldian	Lexington Limestone	Frankfort
37.5	1.56	-5.09	<i>tenuis</i>	Chatfieldian	Lexington Limestone	Frankfort
39	0.13	-5.92	<i>tenuis</i>	Chatfieldian	Lexington Limestone	Frankfort
39.5	0.16	-5.60	<i>tenuis</i>	Chatfieldian	Lexington Limestone	Frankfort
40	0.03	-6.13	<i>tenuis</i>	Chatfieldian	Lexington Limestone	Frankfort
40.7	0.62	-5.92	<i>tenuis</i>	Chatfieldian	Lexington Limestone	Minerva core
41.3	0.70	-5.77	<i>tenuis</i>	Chatfieldian	Lexington Limestone	Minerva core
41.9	0.71	-5.59	<i>tenuis</i>	Chatfieldian	Lexington Limestone	Minerva core
42.5	0.02	-5.06	<i>tenuis</i>	Chatfieldian	Lexington Limestone	Minerva core
42.8	0.64	-5.17	<i>tenuis</i>	Chatfieldian	Lexington Limestone	Minerva core
43.4	0.63	-5.68	<i>tenuis</i>	Chatfieldian	Lexington Limestone	Minerva core
44	0.72	-5.65	<i>tenuis</i>	Chatfieldian	Lexington Limestone	Minerva core
44.6	0.24	-5.99	<i>tenuis</i>	Chatfieldian	Lexington Limestone	Minerva core
45.2	0.19	-5.99	<i>tenuis</i>	Chatfieldian	Lexington Limestone	Minerva core
45.5	0.56	-4.97	<i>tenuis</i>	Chatfieldian	Lexington Limestone	Minerva core
46.1	0.38	-5.60	<i>tenuis</i>	Chatfieldian	Lexington Limestone	Minerva core
46.7	0.69	-5.59	<i>tenuis</i>	Chatfieldian	Lexington Limestone	Minerva core
47.3	0.52	-5.89	<i>tenuis</i>	Chatfieldian	Lexington Limestone	Minerva core
47.9	0.53	-4.65	<i>tenuis</i>	Chatfieldian	Lexington Limestone	Minerva core
48.5	0.43	-5.44	<i>tenuis</i>	Chatfieldian	Lexington Limestone	Minerva core
49.1	0.76	-4.91	<i>tenuis</i>	Chatfieldian	Lexington Limestone	Minerva core
49.7	0.59	-5.58	<i>tenuis</i>	Chatfieldian	Lexington Limestone	Minerva core
50.3	0.75	-5.25	<i>tenuis</i>	Chatfieldian	Lexington Limestone	Minerva core
50.9	1.35	-4.75	<i>tenuis</i>	Chatfieldian	Lexington Limestone	Minerva core
51.2	0.42	-6.03	<i>tenuis</i>	Chatfieldian	Lexington Limestone	Minerva core
51.8	0.41	-5.92	<i>tenuis</i>	Chatfieldian	Lexington Limestone	Minerva core
52.4	0.88	-4.12	<i>tenuis</i>	Chatfieldian	Lexington Limestone	Minerva core
53	0.37	-5.81	<i>tenuis</i>	Chatfieldian	Lexington Limestone	Minerva core
53.6	1.32	-5.18	<i>tenuis</i>	Chatfieldian	Lexington Limestone	Minerva core
55.1	0.75	-5.71	<i>tenuis</i>	Chatfieldian	Lexington Limestone	Minerva core
55.7	0.06	-6.81	<i>tenuis</i>	Chatfieldian	Lexington Limestone	Minerva core
56.9	0.34	-6.43	<i>tenuis</i>	Chatfieldian	Lexington Limestone	Minerva core
59	0.27	-6.57	<i>tenuis</i>	Chatfieldian	Lexington Limestone	Minerva core
59.6	0.25	-4.50	<i>tenuis</i>	Chatfieldian	Lexington Limestone	Minerva core
62	0.34	-5.78	<i>tenuis</i>	Chatfieldian	Lexington Limestone	Minerva core

(continued on next page)

Table 2 (continued)

Meters	$\delta^{13}\text{C}$	$\delta^{18}\text{O}$	Conodont zone	Stage	Formation	Section
63.5	0.21	−5.42	<i>tenuis</i>	Chatfieldian	Lexington Limestone	Minerva core
65	−0.06	−5.98	<i>tenuis</i>	Chatfieldian	Lexington Limestone	Minerva core
65.6	0.10	−5.14	<i>tenuis</i>	Chatfieldian	Lexington Limestone	Minerva core
67.4	0.12	−4.99	<i>tenuis</i>	Chatfieldian	Lexington Limestone	Minerva core
74	−0.89	−5.46	<i>confluens</i>	Chatfieldian	Lexington Limestone	Minerva core
75.8	−0.92	−6.56	<i>confluens</i>	Chatfieldian	Lexington Limestone	Minerva core
76.7	−0.54	−5.03	<i>confluens</i>	Chatfieldian	Lexington Limestone	Minerva core
78.2	−0.65	−5.72	<i>confluens</i>	Chatfieldian	Lexington Limestone	Minerva core
80.3	−0.61	−5.54	<i>confluens</i>	Chatfieldian	Point Pleasant	Minerva core

most reliable component for stable isotope analysis because of its original low magnesium calcite composition. In the studied sections (this paper) brachiopods are not continuously available for high-resolution chemostratigraphy. However, micritic (fine-grained) components are a reproducible, reliable alternative for $\delta^{13}\text{C}$ analysis (Kump et al., 1999; Saltzman, 2001; Saltzman et al., 2004). Several authors (Magaritz, 1983; Banner and Hanson, 1990; among others) have demonstrated that $\delta^{13}\text{C}$ values are largely rock-buffered during the diagenetic histories that commonly affect marine carbonates.

Micrite and brachiopod calcite based $\delta^{13}\text{C}$ curves yield similar trends that are reproducible across continents using biostratigraphy and/or event stratigraphy (i.e. K-bentonites). This demonstrates that it is possible to use micritic components for high-resolution chemostratigraphy. Studies demonstrating this reliability include work done in the Late Ordovician (Gao et al., 1996; Ainsaar et al., 1999; Railsback et al., 2003) as well as other studies throughout the Paleozoic. Several Paleozoic positive $\delta^{13}\text{C}$ excursions have been documented in a wide variety of lithologies from several different continents. For example, the Upper Cambrian (Steptoean Stage) SPICE of +5.0‰ has been recorded on four continents in a variety of lithologies, including dolomite (Glumac and Walker, 1998; Saltzman et al., 1998, 2000). The Upper Ordovician (Hirnantian) positive $\delta^{13}\text{C}$ excursion of +6.0‰ has also been recorded in a variety of lithofacies and is widely documented in North America and Europe (Bergström et al., 2003; Brenchley et al., 1994, 1995, 2003; Finney et al., 1999; Kaljo et al., 2001; Long, 1993). Another example is the Silurian–Devonian boundary, which is associated with a large positive $\delta^{13}\text{C}$ excursion on three different

continents (Andrew et al., 1994; Buggisch, 2001; Hladikova et al., 1997; Saltzman, 2002). Despite the good potential for reliable micrite based $\delta^{13}\text{C}$ curves, diagenetic alteration is still a concern, particularly in heterogeneous carbonates in shallowing-upward successions that are capped by subaerial exposure surfaces. These exposure surfaces have been demonstrated to show an abrupt, negative $\delta^{13}\text{C}$ shift within a meter or less of an exposure horizon, apparently due to influence of meteoric waters that are ^{13}C -poor from surface organic input (Railsback et al., 2003).

Within our sampled sections that record the GICE on the carbonate platform of eastern and central North America, unconformities which could represent exposure surfaces are not common and have only been documented in Kentucky and Oklahoma (Finney, 1986; Holland and Patzkowsky, 1996). $\delta^{13}\text{C}$ values appear to be minimally affected by the unconformities and any associated meteoric waters related to subaerial exposure events in our study sections. Pre-excursion $\delta^{13}\text{C}$ values that occur above and below the unconformities do not exceed a variance of $\leq \pm 1.0\%$ from the established baselines and there are no subaerial exposure surfaces in post-excursion strata sampled for this study.

4. Carbon isotope stratigraphy

4.1. Fittstown, Arbuckle Mountains, southern Oklahoma

A continuous series of samples was collected from a section exposing Bromide and Viola Springs Formations along a roadcut 3.3 miles south of Fittstown, in Pontotoc County, Oklahoma (Fig. 2).

The Fittstown section (thickness of ~75 m) is well studied and unique in that it provides both graptolite biostratigraphy (Finney, 1986) and conodont biostratigraphy (Sweet, 1983). The Bromide and Viola Springs Formations at Fittstown are within the upper *P. undatus* through lower *B. confluens* Conodont Zones and within the upper *C. bicornis* through lower *C. spiniferus* Graptolite Zones (Fig. 3). The basal ~10 m of the outcrop expose bioturbated lime mudstone and wackestones of the Bromide Formation, with an erosional surface at the top and 0.2 m of tan, graptolitic shale of the Viola Springs Formation resting on top of the unconformity.

$\delta^{13}\text{C}$ values (Table 1) in the lower exposed portion of the Bromide Formation start near 0.0‰ with little fluctuation ($\geq \pm 0.5\text{‰}$) up to the top of the formation (Fig. 3). Above, in the cherty lime mudstones–packstone facies of the Viola Springs Formation, $\delta^{13}\text{C}$ values shift to +1.0‰ and become increasingly negative to the top of the cherty limestone facies, with small fluctuations ($\geq \pm 0.5\text{‰}$) reaching low values of –1.5‰. $\delta^{13}\text{C}$ values then swing positive to values of +0.5‰ close to the first occurrence of the conodont *P. tenuis*, ~26 m above the base of the section. $\delta^{13}\text{C}$ values become increasingly positive through the skeletal packstone/grainstone facies, with a peak of

+1.5‰. $\delta^{13}\text{C}$ values then fall back to between 0.0 to –1.0‰ in a lime mudstone–skeletal wackestone facies within the Viola Springs Formation. These post-excursion values coincide with the first occurrence of the conodont *B. confluens*, ~65 m above the base of the section.

4.2. Eastern Laurentia sections

4.2.1. Boonsborough, Frankfort, and Minerva core, north-central Kentucky

Many biostratigraphic (Bergström and Sweet, 1966; Votaw, 1971; Sweet et al., 1974; Sweet, 1979; Richardson and Bergström, 2003), sequence stratigraphic (Holland and Patzkowsky, 1996; Pope and Read, 1997, 1998), and event stratigraphic (Kolata et al., 1996) studies have been published on the Middle and Upper Ordovician carbonates of north-central Kentucky. Upper Turinian through lower Edenian carbonates and shales were sampled from two roadcut exposures near the towns of Frankfort and Boonsborough and one drill core from near the town of Minerva (Fig. 4). These three sections were compiled into a ~120 m thick composite section for north-central Kentucky (Fig. 5). Conodont biostratigraphic studies of these carbonates (Votaw, 1971; Sweet et al.,

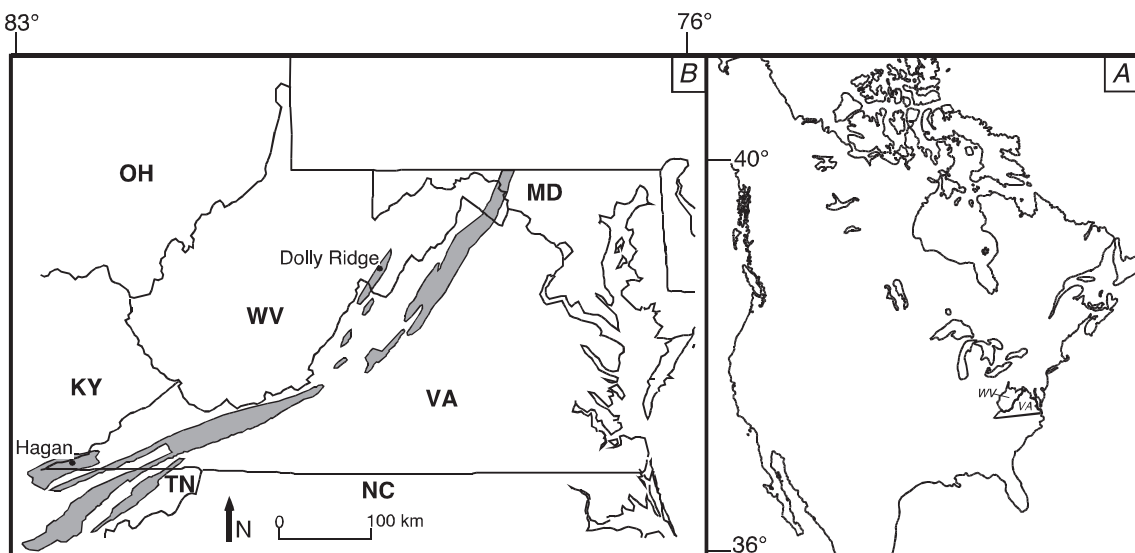


Fig. 6. (A) Map of North America showing an outline of Virginia and West Virginia (VA, WV). (B) Locality map showing Ordovician outcrops in the southern and central Appalachian Basin Region with positions of carbon isotope sampling localities near Hagan, Virginia, and Dolly Ridge, West Virginia.

Table 3
Stable isotope data, Hagan, Virginia

Meters*	$\delta^{13}\text{C}$	$\delta^{18}\text{O}$	Conodont zone	Stage	Formation	Lithology
85	0.65	−4.00	<i>undatus</i>	Turinian	Eggleston	skelatal wackestone
85.5	1.39	−3.81	<i>undatus</i>	Turinian	Eggleston	skelatal wackestone
86	0.43		<i>undatus</i>	Turinian	Eggleston	skelatal wackestone
87	0.63	−3.86	<i>undatus</i>	Chatfieldian	Eggleston	skelatal wackestone
87.5	0.27	−3.87	<i>undatus</i>	Chatfieldian	Eggleston	skelatal wackestone
88	0.24	−5.04	<i>undatus</i>	Chatfieldian	Eggleston	skelatal wackestone
88.5	0.47	−4.57	<i>undatus</i>	Chatfieldian	Eggleston	skelatal wackestone
89	0.44	−4.55	<i>undatus</i>	Chatfieldian	Eggleston	skelatal wackestone
89.5	0.41	−5.58	<i>undatus</i>	Chatfieldian	Eggleston	skelatal wackestone
90	0.50	−5.09	<i>undatus</i>	Chatfieldian	Trenton	skelatal packstone
90.5	−0.01	−5.07	<i>undatus</i>	Chatfieldian	Trenton	skelatal packstone
91	0.14	−5.42	<i>undatus</i>	Chatfieldian	Trenton	skelatal packstone
91.5	−0.06	−6.27	<i>undatus</i>	Chatfieldian	Trenton	skelatal packstone
92	0.47	−4.86	<i>tenuis?</i>	Chatfieldian	Trenton	skelatal packstone
92.5	0.03	−6.13	<i>tenuis?</i>	Chatfieldian	Trenton	skelatal packstone
93	0.62	−5.16	<i>tenuis?</i>	Chatfieldian	Trenton	skelatal packstone
93.5	0.32	−5.40	<i>tenuis?</i>	Chatfieldian	Trenton	skelatal packstone
94	0.46	−5.14	<i>tenuis?</i>	Chatfieldian	Trenton	skelatal packstone
94.5	0.56	−5.42	<i>tenuis?</i>	Chatfieldian	Trenton	skelatal packstone
95	0.48	−5.44	<i>tenuis?</i>	Chatfieldian	Trenton	skelatal packstone
95.5	0.53	−5.16	<i>tenuis?</i>	Chatfieldian	Trenton	skelatal packstone
96	0.80	−4.97	<i>tenuis?</i>	Chatfieldian	Trenton	skelatal packstone
96.5	0.55	−5.39	<i>tenuis?</i>	Chatfieldian	Trenton	skelatal packstone
97	0.28	−5.03	<i>tenuis?</i>	Chatfieldian	Trenton	skelatal packstone
97.5	0.61	−4.90	<i>tenuis?</i>	Chatfieldian	Trenton	skelatal packstone
98	0.62	−4.85	<i>tenuis?</i>	Chatfieldian	Trenton	skelatal packstone
98.5	0.46	−5.12	<i>tenuis?</i>	Chatfieldian	Trenton	skelatal packstone
99	0.42	−6.25	<i>tenuis?</i>	Chatfieldian	Trenton	skelatal packstone
99.5	0.70	−5.39	<i>tenuis?</i>	Chatfieldian	Trenton	skelatal packstone
100	0.44	−5.36	<i>tenuis?</i>	Chatfieldian	Trenton	skelatal packstone
100.5	0.56	−5.39	<i>tenuis?</i>	Chatfieldian	Trenton	skelatal packstone
101	0.45	−5.04	<i>tenuis?</i>	Chatfieldian	Trenton	skelatal packstone
101.5	0.30	−5.04	<i>tenuis?</i>	Chatfieldian	Trenton	skelatal packstone
102	0.33	−5.29	<i>tenuis?</i>	Chatfieldian	Trenton	skelatal packstone
102.5	0.66	−4.87	<i>tenuis?</i>	Chatfieldian	Trenton	skelatal packstone
103	0.86	−4.70	<i>tenuis?</i>	Chatfieldian	Trenton	skelatal packstone
103.5	0.71	−5.12	<i>tenuis?</i>	Chatfieldian	Trenton	skelatal packstone
104	0.63	−5.33	<i>tenuis?</i>	Chatfieldian	Trenton	skelatal packstone
104.5	0.58	−4.88	<i>tenuis?</i>	Chatfieldian	Trenton	skelatal packstone
105	0.73	−5.13	<i>tenuis?</i>	Chatfieldian	Trenton	skelatal packstone
105.5	0.67	−4.78	<i>tenuis?</i>	Chatfieldian	Trenton	skelatal packstone
106	0.71	−5.22	<i>tenuis?</i>	Chatfieldian	Trenton	skelatal packstone
106.5	1.18	−4.65	<i>tenuis?</i>	Chatfieldian	Trenton	skelatal packstone
107	0.33	−4.95	<i>tenuis?</i>	Chatfieldian	Trenton	skelatal packstone
107.5	0.82	−5.03	<i>tenuis?</i>	Chatfieldian	Trenton	skelatal packstone
108	1.01	−5.60	<i>tenuis?</i>	Chatfieldian	Trenton	skelatal packstone
108.5	0.75	−5.52	<i>tenuis?</i>	Chatfieldian	Trenton	skelatal packstone
109	0.75	−5.54	<i>tenuis?</i>	Chatfieldian	Trenton	skelatal packstone
109.5	0.10	−5.80	<i>tenuis</i>	Chatfieldian	Trenton	skelatal packstone
110	0.41	−5.32	<i>tenuis</i>	Chatfieldian	Trenton	skelatal packstone
110.5	1.09	−5.11	<i>tenuis</i>	Chatfieldian	Trenton	skelatal packstone
111	0.83	−5.77	<i>tenuis</i>	Chatfieldian	Trenton	skelatal packstone
111.5	0.66	−5.65	<i>tenuis</i>	Chatfieldian	Trenton	skelatal packstone

Table 3 (continued)

Meters*	$\delta^{13}\text{C}$	$\delta^{18}\text{O}$	Conodont zone	Stage	Formation	Lithology
112	1.07	−4.96	<i>tenuis</i>	Chatfieldian	Trenton	skelteal packstone
123	0.75	−6.15	<i>tenuis</i>	Chatfieldian	Trenton	skeletal grainstone
125	2.12	−4.75	<i>tenuis</i>	Chatfieldian	Trenton	skelteal packstone
127	2.14	−4.89	<i>tenuis</i>	Chatfieldian	Trenton	skeletal grainstone
129	1.58	−4.34	<i>tenuis</i>	Chatfieldian	Trenton	skeletal grainstone
131	1.3	−5.4	<i>tenuis</i>	Chatfieldian	Trenton	skeletal wackestone
134	2.38	−5.04	<i>tenuis</i>	Chatfieldian	Trenton	lime mudstone
135	2.79	−4.48	<i>tenuis</i>	Chatfieldian	Trenton	lime mudstone
136	1.96	−4.73	<i>tenuis</i>	Chatfieldian	Trenton	lime mudstone
139	1.51	−4.8	<i>tenuis</i>	Chatfieldian	Trenton	skeletal grainstone
143	1.34	−4.88	<i>tenuis</i>	Chatfieldian	Trenton	skeletal grainstone
147.0	2.01	−5.19	<i>tenuis</i>	Chatfieldian	Trenton	skeletal wackestone
150.5	2.46	−5.21	<i>tenuis</i>	Chatfieldian	Trenton	lime mudstone
155.0	1.71	−4.25	<i>tenuis</i>	Chatfieldian	Trenton	skeletal grainstone
159.0	2.21	−4.48	<i>tenuis</i>	Chatfieldian	Trenton	skeletal grainstone
161.5	2.23	−4.91	<i>tenuis</i>	Chatfieldian	Trenton	skelteal packstone
163.0	2.81	−4.95	<i>tenuis</i>	Chatfieldian	Trenton	lime mudstone
164.5	1.86	−4.74	<i>tenuis</i>	Chatfieldian	Trenton	lime mudstone
167.0	1.25	−4.89	<i>tenuis</i>	Chatfieldian	Trenton	skeletal wackestone
169.5	2.46	−5.28	<i>tenuis</i>	Chatfieldian	Trenton	lime mudstone
171.0	2.46	−4.22	<i>tenuis</i>	Chatfieldian	Trenton	skeletal grainstone
173.5	2.34	−4.63	<i>tenuis</i>	Chatfieldian	Trenton	lime mudstone
175.0	1.19	−5.05	<i>tenuis</i>	Chatfieldian	Trenton	skeletal grainstone
179.0	0.91	−5.74	<i>tenuis</i>	Chatfieldian	Trenton	skeletal grainstone
182.5	1.86	−3.81	<i>tenuis</i>	Chatfieldian	Trenton	skelteal packstone
184.5	1.38	−5.13	<i>tenuis</i>	Chatfieldian	Trenton	skeletal grainstone
254.0	0.91	−3.84	<i>tenuis</i>	Chatfieldian	Trenton	skeletal wackestone
258.0	0.08	−4.28	<i>tenuis</i>	Chatfieldian	Trenton	skeletal wackestone
262.0	0.22	−4.04	<i>tenuis</i>	Chatfieldian	Trenton	lime mudstone
268.0	0.31	−3.91	<i>tenuis</i>	Chatfieldian	Trenton	lime mudstone
272.0	−1.01	−4.44	<i>confluens</i>	Chatfieldian	Trenton	skelteal packstone
276.0	−1.11	−4.81	<i>confluens</i>	Chatfieldian	Trenton	skelteal packstone
280.0	−1.27	−4.81	<i>confluens</i>	Chatfieldian	Trenton	skeletal grainstone
284.0	−0.51	−4.55	<i>confluens</i>	Chatfieldian	Trenton	skelteal packstone

* Section begins 86 m below the Millbrig K-bentonite bed in the Eggleston Limestone.

1974; Sweet, 1979; Richardson and Bergström, 2003) demonstrate that the upper Tyrone through lower Kope Formations are within the *P. undatus* through *B. confluens* Zones. The upper Tyrone Formation consists of bioturbated lime mudstones, skeletal wackestones, and occasional pelletal grainstones and is referable to the *P. undatus* Zone. An erosional surface marking the top of the Tyrone Formation is overlain by skeletal grainstones of the Lexington Limestone.

$\delta^{13}\text{C}$ values (Table 2) in the upper Tyrone Formation begin near 0.0‰ and trend towards +1.0‰ just below the Deicke K-bentonite bed (Fig. 5). Above the Deicke $\delta^{13}\text{C}$ values are 0.0‰ and trending to +1.0‰ through the Tyrone/Lexington

Limestone contact. Values within skeletal grainstones of the Curdsville Member rise gradually with fluctuations of $\delta^{13}\text{C} \geq \pm 1.0\text{‰}$ near the *P. undatus*/*P. tenuis* zonal boundary. In the overlying interbedded shales and skeletal wackestones and packstones of the Logana Member, $\delta^{13}\text{C}$ values quickly shift towards heavier, reaching as high as +2.8‰ within the *P. tenuis* Zone. The skeletal packstones and grainstones of the lower Grier, Macedonia, and upper Grier members have $\delta^{13}\text{C}$ values $\sim +1.0\text{‰}$ with fluctuations of $\geq \pm 1.0\text{‰}$. $\delta^{13}\text{C}$ values gradually fall back to pre-excursion values through the upper Logana, lower Grier, and Macedonia members of the Lexington Limestone. Within the upper Grier Member, near the *P. tenuis*/*B. confluens* zonal boundary, $\delta^{13}\text{C}$ values

shift from near 0.0‰ to pre-excursion values of $-1.0‰$.

4.2.2. Hagan, Southern Appalachians, southwestern Virginia

In Lee County, Virginia, Middle to Upper Ordovician strata exposed in a railroad cut at Hagan (Fig. 6) have been very well studied (Fetzer, 1973; Hall, 1986; Bergström et al., 1988; Haynes, 1992, 1994; Leslie, 1995; Kolata et al., 1996; Mitchell et al., 2004). Samples for $\delta^{13}\text{C}$ analyses were collected from the upper Eggleston Limestone to the top of the Trenton Limestone (~220 m). Studies by Fetzer (1973), Hall (1986), and Bergström et al. (1988) show that the Upper Ordovician Eggleston and Trenton Limestones in this section are within the *P. undatus* through *P. tenuis* Conodont Zones.

Haynes (1992, 1994), Kolata et al. (1996), and Mitchell et al. (2004) have studied the K-bentonites at Hagan extensively and the Deicke, Millbrig, V-7, and House Springs K-bentonites are present within this sampled section. The Eggleston Limestone is predominantly bioturbated lime mudstones and wackestones. The Trenton Limestone is mainly thin-medium bedded skeletal packstones/grainstones with thin shale interbeds.

In the Eggleston, $\delta^{13}\text{C}$ values (Table 3) start at $+0.9‰$ but fall to near $-0.0‰$ 3 m above the Millbrig K-bentonite in the Trenton Limestone. $\delta^{13}\text{C}$ values in the Trenton become increasingly positive through the packstone/grainstones (although there are high frequency $\delta^{13}\text{C}$ fluctuations ($\geq \pm 1.0‰$)), with peak values $+2.8‰$ in the *P. tenuis* Zone, ~76 m above the Millbrig K-bentonite bed (Fig. 7). The heavy $\delta^{13}\text{C}$

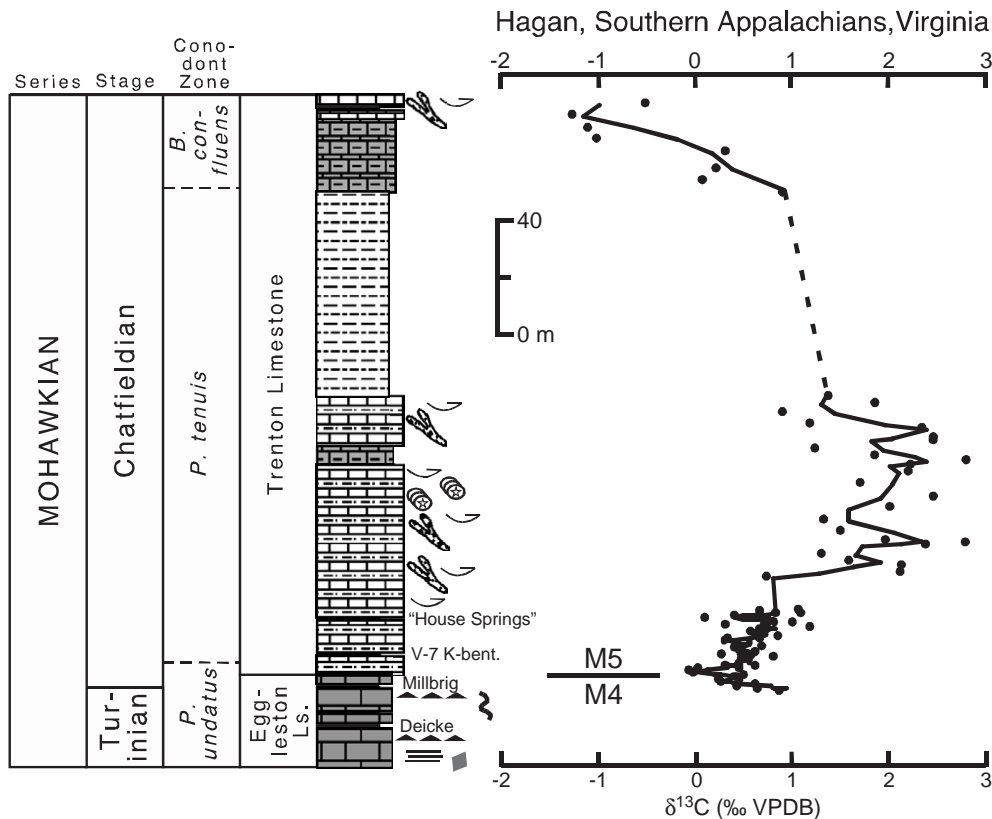


Fig. 7. $\delta^{13}\text{C}$ plots from the Hagan section, southern Appalachians, Virginia. Due to the high frequency fluctuations of $\delta^{13}\text{C}$ values a three point running average was plotted (line drawn between data points) to reflect the overall trend of $\delta^{13}\text{C}$ values through this section. Conodont biostratigraphy based on Bergström et al. (1988) and Leslie (1995). K-bentonite event stratigraphy from Kolata et al. (1996) and Mitchell et al. (2004).

values in the Trenton interval are fluctuating between 1.8‰ and 2.8‰ possibly because of the heterogeneous nature (skeletal grainstones) of the samples. The lower Trenton samples fluctuate on a smaller frequency ($\geq 0.5\%$), possibly due to the greater presence of micritic components (wackestones, packstones) in the samples relative to the upper Trenton Limestone. Just below a large covered interval, $\delta^{13}\text{C}$ values at ~93 m above the Millbrig are 1.4‰ and possibly returning to pre-excursion values. Above the covered, predominantly shale interval, is the *P. tenuis*/*B. confluens* zonal boundary. $\delta^{13}\text{C}$ values are at +1.0‰ and trend more negative toward the Trenton/

Reedsville Shale contact with the uppermost Trenton $\delta^{13}\text{C}$ values of -0.5 to -1.5‰.

4.2.3. Dolly Ridge, Central Appalachians, West Virginia

The type section for the Dolly Ridge Formation was sampled from an outcrop along a farm road on Dolly Ridge 0.8 miles southeast of Riverton, in Pendleton County, West Virginia (Fig. 6). The ~180 m thick exposure of Nealmont Limestone through lower Reedsville Formation (Fig. 8) was first described by Perry (1972). Perry (1972) also documented 14 K-bentonites within this section,

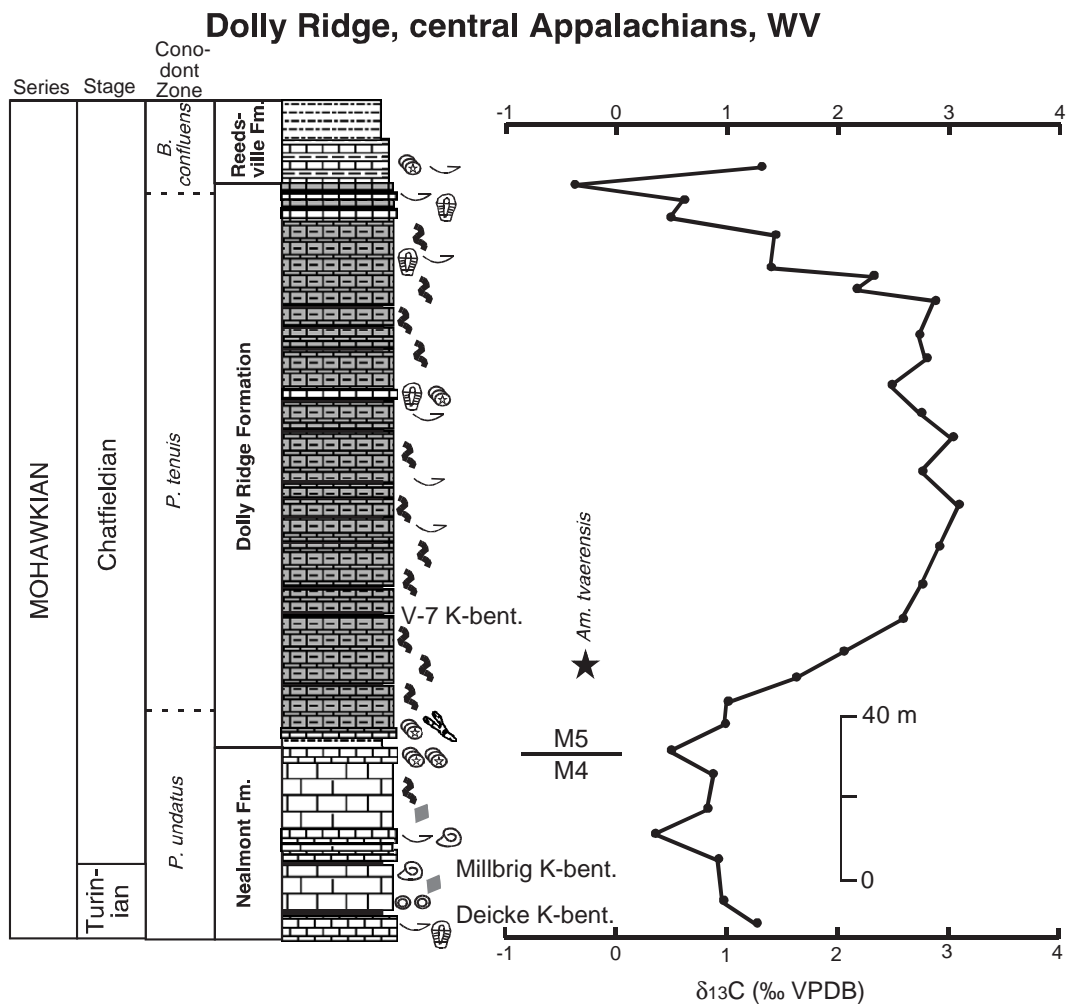


Fig. 8. $\delta^{13}\text{C}$ plots from the Dolly Ridge section, central Appalachians, West Virginia with conodont biostratigraphy based on Keith (1989), and Keith and Hall (1989). K-bentonite event stratigraphy plotted from Perry (1972), and Haynes (personal communication).

the lower two being the thickest and these are most likely the Deicke and Millbrig K-bentonites, respectively (Haynes, personal communication). Because of the limited biostratigraphic studies done so far on the Dolly Ridge Formation from nearby sections in German Valley (Keith, 1989; Keith and Hall, 1989), fourteen samples were collected from the Dolly Ridge section and processed for conodonts as part of this study. These samples show that most of the Dolly Ridge Formation lies within the upper *P. undatus* and the *P. tenuis* Zones with the uppermost beds of the Dolly Ridge Formation representing the basal *B. confluens* Zone (Keith, 1989; Keith and Hall, 1989). The Nealmont Limestone consists of predominantly bioturbated lime mudstones and wackestones, with occasional skeletal packstones/grainstones. The Dolly Ridge Formation consists of

interbedded dark gray–black bioturbated lime mudstones and shales, with an occasional skeletal packstone.

The $\delta^{13}\text{C}$ values (Table 4) in the Nealmont Limestone, in the *P. undatus* Zone and just below the Deicke K-bentonite bed, begin at +1.0‰. Above the Millbrig K-bentonite bed $\delta^{13}\text{C}$ values stay between 0.0‰ and +0.8‰ through the crinoidal packstones at the top of the Nealmont but shift towards +1.0‰ across the Nealmont/Dolly Ridge Formation contact. $\delta^{13}\text{C}$ values in the lower Dolly Ridge continue to rise with the heaviest values reaching +3.2‰ in the *P. tenuis* Zone, ~87 m above the Millbrig K-bentonite bed. $\delta^{13}\text{C}$ values are between +3.2‰ to +2.7‰ for ~48 m, within the Dolly Ridge Formation, and then fall back to pre-excursion values. $\delta^{13}\text{C}$ values shift from +2.0‰ to –0.4‰ in the uppermost Dolly Ridge

Table 4
Stable isotope data, Dolly Ridge, West Virginia

Meters	$\delta^{13}\text{C}$	$\delta^{18}\text{O}$	Conodont zone	Stage	Formation	Lithology
0	1.26	–4.45	<i>undatus</i>	Turinian	Nealmont	skeletal packstone
5.1	0.96	–5.74	<i>undatus</i>	Turinian	Nealmont	lime mudstone
15.1	0.92	–5.33	<i>undatus</i>	Turinian	Nealmont	skeletal packstone
21.1	0.36	–5.63	<i>undatus</i>	Chatfieldian	Nealmont	skeletal wackestone
27.1	0.82	–5.92	<i>undatus</i>	Chatfieldian	Nealmont	lime mudstone
35.6	0.88	–5.93	<i>undatus</i>	Chatfieldian	Nealmont	lime mudstone
41	0.49	–6.07	<i>undatus</i>	Chatfieldian	Nealmont	skeletal packstone
47.5	0.98	–6.12	<i>tenuis?</i>	Chatfieldian	Dolly Ridge	lime mudstone
52.5	1.01	–5.81	<i>tenuis?</i>	Chatfieldian	Dolly Ridge	lime mudstone
58.5	1.61	–5.88	<i>tenuis</i>	Chatfieldian	Dolly Ridge	lime mudstone
64.5	2.05	–5.78	<i>tenuis</i>	Chatfieldian	Dolly Ridge	lime mudstone
72.5	2.58	–6.02	<i>tenuis</i>	Chatfieldian	Dolly Ridge	lime mudstone
80.5	2.75	–6.03	<i>tenuis</i>	Chatfieldian	Dolly Ridge	lime mudstone
89.5	2.90	–5.95	<i>tenuis</i>	Chatfieldian	Dolly Ridge	lime mudstone
99.5	3.09	–5.71	<i>tenuis</i>	Chatfieldian	Dolly Ridge	lime mudstone
107.5	2.76	–5.89	<i>tenuis</i>	Chatfieldian	Dolly Ridge	lime mudstone
115.5	3.02	–5.99	<i>tenuis</i>	Chatfieldian	Dolly Ridge	lime mudstone
121.5	2.75	–6.24	<i>tenuis</i>	Chatfieldian	Dolly Ridge	lime mudstone
128.2	2.48	–6.32	<i>tenuis</i>	Chatfieldian	Dolly Ridge	lime mudstone
134.2	2.79	–6.16	<i>tenuis</i>	Chatfieldian	Dolly Ridge	lime mudstone
140.2	2.74	–5.65	<i>tenuis</i>	Chatfieldian	Dolly Ridge	skeletal packstone
148.2	2.87	–6.56	<i>tenuis</i>	Chatfieldian	Dolly Ridge	lime mudstone
151.2	2.17	–6.21	<i>tenuis</i>	Chatfieldian	Dolly Ridge	lime mudstone
154.2	2.32	–6.26	<i>tenuis</i>	Chatfieldian	Dolly Ridge	lime mudstone
156.2	1.39	–6.28	<i>tenuis</i>	Chatfieldian	Dolly Ridge	skeletal wackestone
164.2	1.44	–7.02	<i>tenuis</i>	Chatfieldian	Dolly Ridge	lime mudstone
168.2	0.50	–6.82	<i>tenuis</i>	Chatfieldian	Dolly Ridge	skeletal wackestone
172.2	0.62	–6.13	<i>tenuis</i>	Chatfieldian	Dolly Ridge	skeletal wackestone
176.2	–0.37	–6.66	<i>confluens?</i>	Chatfieldian	Dolly Ridge	lime mudstone
180.2	1.29	–7.43	<i>confluens?</i>	Chatfieldian	Dolly Ridge	skeletal packstone

Formation near the gradational contact with the Reedsville Formation and the *P. tenuis/B. confluens* zonal boundary.

5. Discussion

All four Mohawkian successions examined record the Guttenberg $\delta^{13}\text{C}$ excursion (GICE) and confirm the regional significance of this paleoceanographic event. However, the excursion in Oklahoma does not reach peak $\delta^{13}\text{C}$ values as high as in the eastern Laurentian sections. These peak $\delta^{13}\text{C}$ values in Oklahoma also follow lithologic evidence for upwelling. Here we interpret the observed local variations in $\delta^{13}\text{C}$ and lithofacies shifts in the context of the regional aquafacies model of Holmden et al. (1998). We then focus on the implications of the new $\delta^{13}\text{C}$ curves presented for oceanographic models of organic carbon production and burial, as well as sea-level, during the Late Ordovician.

5.1. Local variations in the $\delta^{13}\text{C}$ excursion

The $>1.0\text{‰}$ offset in the GICE values from Fittstown, Oklahoma to the Appalachian Foreland Basin could reflect a combination of biological (nutrient dependent) and thermodynamic (temperature dependent) processes that govern the variance of $\delta^{13}\text{C}$ of dissolved inorganic carbon (Kroopnick, 1985; Gruber et al., 1999). The modern tropical–subtropical open oceans only differ by $\sim 0.5\text{‰}$ (Gruber et al., 1999), and the largest marginal sea, the South China Sea, only differs from the adjacent Pacific ocean by $\leq 0.5\text{‰}$ (Lin et al., 1999). However, the observed regional variations in $\delta^{13}\text{C}$ among the Upper Ordovician aquafacies are comparable to modern carbonate platforms of the Bahamas and Florida Bay (Patterson and Walter, 1994), where there is as much as a 4.0‰ offset in $\delta^{13}\text{C}$ values relative to the open ocean. Holmden et al. (1998) defined three different aquafacies for Mohawkian seas: the Midcontinent aquafacies, Taconic aquafacies, and Southern aquafacies. The GICE in the Midcontinent aquafacies has pre-

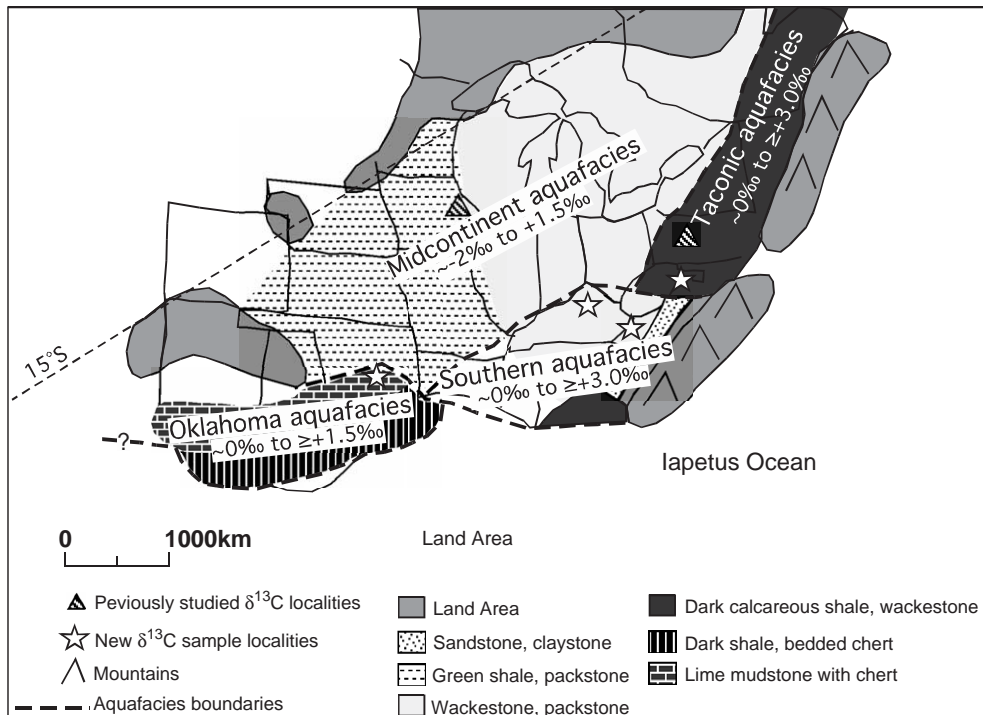


Fig. 9. Late Middle Ordovician paleogeographic reconstruction of eastern Laurentia showing lithofacies, aquafacies (modified from Holmden et al., 1998), and the respective baseline and heaviest $\delta^{13}\text{C}$ values of the GICE for the aquafacies.

GICE values -2‰ and peak values at $+1.5\text{--}2.0\text{‰}$ (Ludvigson et al., 1996; Simo et al., 2003) (Fig. 9). In the Southern and Taconic aquafacies the pre-GICE values are $\sim 0.0\text{‰}$ and peak values are $\sim \geq +3.0\text{‰}$ (Fig. 9). Distribution of different water masses (aquafacies) is the result of thermohaline (density) and wind-driven (wind friction in the surface mixed layer) factors in the Ordovician seas (Wilde, 1991). Surface circulation will transport water masses from areas of formation until a different water mass is encountered, the denser water mass then sinks below the lighter one, thus forming a boundary between the two water masses (Wilde, 1991). Nutrient dependent biological processes are the most likely control on these local $\delta^{13}\text{C}$ variations in the epeiric sea carbonates presented here, which formed in subtropical to tropical waters with a relatively narrow temperature range ($12\text{--}23\text{ }^{\circ}\text{C}$) (Railsback, 1989).

In south-central Oklahoma pre-excursion values based on the three Bromide samples are 0.0‰ , which are different than base lines in the Midcontinent

aquafacies (-1.0‰ to -2.0‰) and closer to the Southern aquafacies ($\sim 0.5\text{‰}$ to $\sim 1.0\text{‰}$). The Trenton transgression (sea-level rise), resulted in the initial deposition of the Viola Springs Formation in Oklahoma, and brought the thermocline up onto the shelf, which allowed for the cool, dense, nutrient-rich (i.e. phosphate, silica), bottom waters to begin upwelling. In addition, or alternatively, global cooling may have altered the thermohaline circulation and promoted more vigorous upwelling in platform margin locations worldwide (Pope and Steffen, 2003). Regardless of the cause, upwelling began during the latest Turinian to earliest Chatfieldian along the southern margin of Laurentia in Oklahoma and adjacent areas (Pope and Steffen, 2003) and in the Sebree Trough where cool waters entered near central Arkansas (Kolata et al., 2001) (Fig. 10). These cool, phosphate and silica-rich waters also brought isotopically lighter carbon up from depth, resulting in lower chert rich Viola Springs Formation $\delta^{13}\text{C}$ values between 0.0‰ and -1.5‰ . This upwelling effect can also be observed in the

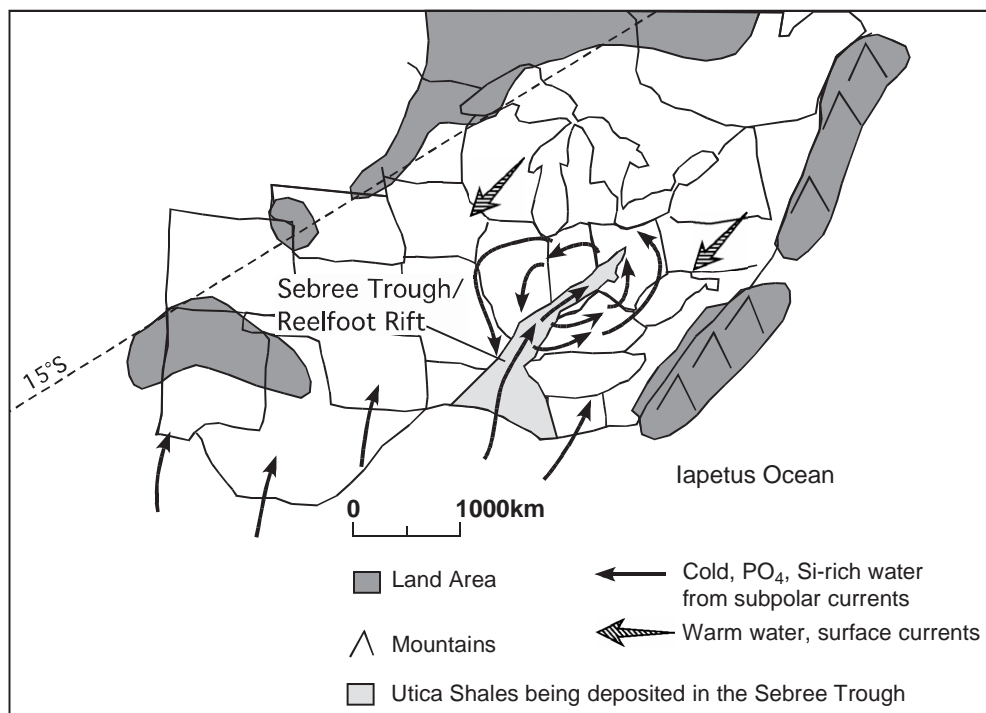


Fig. 10. Late Middle Ordovician paleogeographic reconstruction of eastern Laurentia showing Taconic Mountains forming along the eastern margin of Laurentia, and ocean circulation patterns that were affecting the different water masses in the shallow epeiric seas that covered the Midcontinent of North America (modified from Kolata et al., 2001).

modern seas where in the tropical Pacific isotopically-light deep waters ($\sim 0.5\%$ lighter than waters 15° to the south) are brought to the surface (Gruber et al., 1999). However unlikely, it is not possible to completely rule out incorporation of light carbon through organic matter oxidation during diagenesis.

The Viola Springs Formation contains abundant chert (up to 70% chert) and graptolites, which are further evidence for upwelling in this continental margin setting (Finney and Berry, 1997; Pope and Steffen, 2003). Both primary biogenic and secondary silica are present in the interbedded chert and lime mudstone and wackestones of the lower Viola Springs Formation (Galvin, 1983; Candelaria and Roux, 1997). Chert at the Fittstown, Oklahoma section appears in interbedded discontinuous elongate lenses and irregular nodules, and is interpreted to be primary depositional and early diagenetic chert by Pope (2004). Pope (2004) also interpreted chert from an Interstate 35 outcropping of the Viola Springs Formation to be early diagenetic and this is consistent with our interpretations of chert from the Fittstown section, which is a stratigraphically more complete section of the Viola Springs Formation.

The heaviest values ($+1.5\%$) of the GICE are recorded in the skeletal packstones and grainstones which lack chert in the upper Viola Springs Formation. A likely explanation for this lithofacies change and higher $\delta^{13}\text{C}$ values was a decrease in nutrient (phosphate, silica) delivery, which produced coarser carbonates with no chert and heavier $\delta^{13}\text{C}$ values. Hallock and Schlager (1986) documented that carbonate platforms and associated reef communities thrive in nutrient poor (oligotrophic) waters, and increased nutrient availability (via upwelling, turnover, or runoff from land) decreases water transparency, temperature, and ultimately carbonate production on the platform. Increased nutrient availability, resulting in mesotrophic to eutrophic waters, also increases bioerosion on the carbonate platform resulting in predominantly mud dominated carbonates and hardgrounds forming on the platform (Hallock, 1988). Conversely, oligotrophic waters promote the production of skeletal carbonates and limit the production of carbonate muds (Hallock, 1988). Therefore, we infer that the lower chert and lime mudstone dominated Viola Springs Formation formed in mesotrophic to eutrophic waters, while the (isotopically

heavier) skeletal packstones and grainstones of the upper Viola Springs formed in oligotrophic waters. Similar changes in carbonate lithologies, nutrient availability, as well as faunal changes, have been documented in the Silurian, and an oceanic model involving alternating oceanic episodes (P and S episodes) was proposed by Jeppsson (1990). P episodes are periods where upwelling and terrestrial weathering are prevalent on the carbonate platform, resulting in mesotrophic to eutrophic waters producing argillaceous, finer grained carbonates and shales being deposited on the platform, which may apply to the chert-rich lower Viola Springs. S episodes represent periods of oligotrophic waters on the carbonate platform resulting in deposition of reefal and other skeletal carbonates (Jeppsson, 1990), such as what we observe in the middle part of the Viola Springs Formation that records the GICE.

The GICE in Oklahoma appears to be a net shift of $+1.5\%$ in magnitude, which is half the magnitude of the GICE in the Taconic and Southern aquafacies ($+3.0\%$) (Figs. 5, 7, 8, 11). We attribute this difference in magnitude of the GICE in Oklahoma to the effects of upwelling on local $\delta^{13}\text{C}$ values in carbonates on the Oklahoma ramp. Broecker and Maier-Reimer (1992) discussed an analogous nutrient and carbon isotope relationship in the modern oceans, where surface waters of the Antarctic contain high ($1.6 \mu\text{mol/kg}$) PO_4 and are 1.5% lighter in $\delta^{13}\text{C}$ than tropical surface waters containing lower ($\sim 0.2 \mu\text{mol/kg}$) PO_4 . In summary, the GICE in Oklahoma is recorded in a coarsening-upward succession after a period of enhanced nutrient delivery through upwelling in this continental margin setting (Fig. 11).

5.2. *Upwelling and nutrient flow into the Taconic aquafacies*

The deep, cooler, isotopically lighter oceanic waters that began upwelling in Oklahoma and other regions (e.g. Sebree Trough) were likely the source of the nutrients and cause of the enhanced primary productivity during the GICE (Fig. 10). The isotopically light carbon brought to the surface in Oklahoma was sequestered in the Viola Springs Formation, and in the deeper water deposits of the upper Womble Shale and lower Bigfork Chert (Finney, 1986), and was also sequestered in the Utica Shale of the Sebree

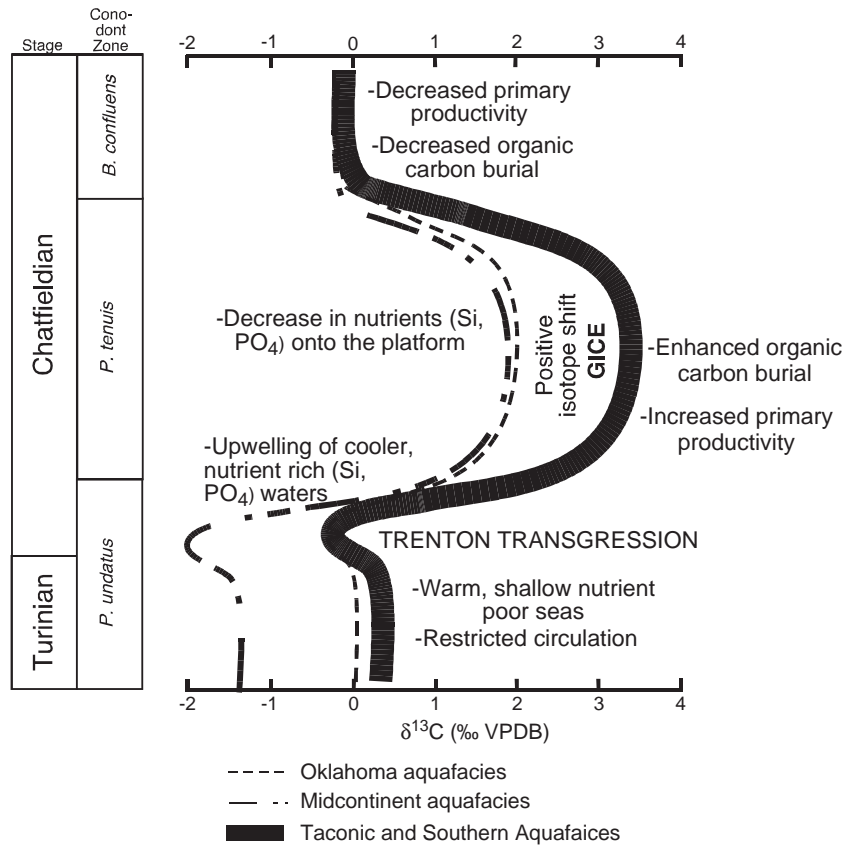


Fig. 11. A model for the Guttenberg Carbon Isotope Excursion (GICE) demonstrating the biostratigraphic and paleoceanographic relations. Also shown is the differing magnitudes of the GICE between the Oklahoma aquafacies (dashed curve) and the Southern and Taconic aquafacies (bold curve).

Trough (Kolata et al., 2001). The resulting ^{13}C -enriched waters were then transported eastwards to the region of the Taconic aquafacies. The GICE is thus recorded with heavier $\delta^{13}\text{C}$ values ($\sim +1.0\text{‰}$ heavier) in the nearby Lexington Limestone in Kentucky, Trenton Limestone in Virginia, and the Hermitage Limestone in Tennessee (Railsback et al., 2003). The heaviest values are recorded in sections in Pennsylvania ($+0.5\text{‰}$ to $+1.0\text{‰}$ heavier; Patzkowsky et al., 1997) that were furthest from the source of upwelled waters and were increasingly nutrient depleted.

Upwelling as a source of nutrients for the enhanced organic carbon burial that caused the GICE is consistent with cherty units in Oklahoma, which are correlated with other Upper Ordovician cherty units along the southern margins of Laurentia.

These units are thought to record a long-lived, widespread upwelling event in a Late Ordovician period of more vigorous deep ocean circulation produced by the onset of cooling and glaciation of Gondwana (Pope, 2004). The record of sea level in the Oklahoma region is consistent with this model. In Oklahoma the major eustatic rise in sea-level (the Trenton Transgression of Holland and Patzkowsky (1996)) is shown by the abrupt contact between the shallow water, tropical-type carbonates of the upper Bromide Formation and the overlying deeper water, temperate-type carbonates of the lower Viola Springs Formation. After this major transgressive event, sea-level appeared to fall, as indicated by a coarsening and increase of skeletal grains upwards through the Viola Springs Formation (Finney, 1986). In addition, conodont faunas support this change in water depths

in that the lower parts of the Viola Springs Formation (Sweet, 1983) are dominated by *P. undatus*, which indicates a deeper water biofacies (Sweet, 1984b; Sweet and Bergström, 1984). Higher up in the Viola Springs Formation *P. tenuis* and *B. confluens* appear/or become more abundant, indicating a shallower water biofacies (Sweet, 1983). Based upon these data it appears that sea-level was falling through the GICE, which would be consistent with sea-level changes during this $\delta^{13}\text{C}$ excursion in Estonia (Ainsaar et al., 1999). Saltzman and Young (2005) interpret a major eustatic Chatfieldian sea-level fall in the passive margin sequence of the western margin of Laurentia (Nevada), and correlate it with regressive events in Baltica (Nielsen, 2004). However, Patzkowsky et al. (1997) interpret the GICE in eastern Laurentia to be associated with a sea-level rise, but this rise in sea-level is likely a local effect due to flexural subsidence in response to the nearby Taconic Orogeny. A sea-level lowering is also consistent with climatic cooling related to enhanced organic carbon burial and a $p\text{CO}_2$ draw-down associated with the GICE (Patzkowsky et al., 1997). Recent models for the Late Ordovician (Herrmann et al., 2004) have shown that drops in sea level, continental drift, atmospheric $p\text{CO}_2$, and changing paleoceanography were necessary conditions for long-term cooling and glaciation in the Late Ordovician.

6. Conclusions

The Guttenberg $\delta^{13}\text{C}$ excursion (GICE) is recognized in the Viola Springs Formation in Oklahoma (maximum $\delta^{13}\text{C}$ values of +1.5‰), the Lexington Limestone in Kentucky (maximum $\delta^{13}\text{C}$ values of +2.8‰), the Trenton Limestone in Virginia (maximum $\delta^{13}\text{C}$ values of +2.8‰), and the Dolly Ridge Formation in West Virginia (maximum $\delta^{13}\text{C}$ values of +3.2‰). The magnitude ($\geq +3.0\text{‰}$) and timing (beginning in the upper *P. undatus* and heaviest values within the *P. tenuis* Conodont Zones) of this $\delta^{13}\text{C}$ excursion have been demonstrated to be the same in all three previously established aquafacies. The excursion occurs above the Millbrig K-bentonite bed, and within the M5 depositional sequence of Holland and Patzkowsky (1996). In this study

variations of heavy $\delta^{13}\text{C}$ values from +1.5‰, to +2.8‰, to +3.2–3.5‰ are shown to occur over the carbonate platform of eastern Laurentia. The $>1.0\text{‰}$ offset in the GICE values from Fittstown, Oklahoma to the Appalachian Foreland Basin does reflect the different water-masses present across the shallow epeiric seas of Laurentia during this time. We interpret the lighter $\delta^{13}\text{C}$ values in Oklahoma compared to other sections as resulting from nutrient rich, isotopically light waters upwelling which caused increased primary productivity along the southern margin of Laurentia and extended into the Sebree Trough. Subsequently, isotopically light carbon was sequestered in these areas, resulting in heavier $\delta^{13}\text{C}$ values in waters that were further circulated onto the carbonate platform. This global perturbation of the carbon cycle thus appears to have regional expression, which is linked to changes in paleoceanography (i.e. upwelling, ocean circulation), organic carbon production, and burial, and as well as sea-level fluctuations.

Acknowledgements

We would like to thank the stable isotopic laboratories at University of Michigan, Texas A & M University, and University of Saskatchewan for analysis of the samples presented in this paper. We would also like to thank Steve Leslie, Jack Hall, John Haynes, Mickey Matthews, Brad Cramer, and Kate Tierney for their help with fieldwork, providing valuable information about sample localities, and/or insightful discussion of this project. We thank the two anonymous reviewers who provided helpful comments and suggestions for this manuscript.

References

- Ainsaar, L., Meidla, T., Martma, T., 1999. Evidence for a widespread carbon isotopic event associated with late Middle Ordovician sedimentological and faunal changes in Estonia. *Geological Magazine* 136 (1), 49–62.
- Alberstadt, L.P., 1973. Articulate brachiopods of the Viola Formation (Ordovician) in the Arbuckle Mountains, Oklahoma. *Oklahoma Geological Survey Bulletin* 117, 1–87.
- Andrew, A.S., Hamilton, P.J., Mawson, R., Talent, J.A., Whitford, D.J., 1994. Isotopic correlation tools in the mid-Paleozoic and

- their relation to extinction events. *Australian Petroleum Exploration Association* 34, 268–277.
- Azmy, K., Veizer, J., Bassett, M.G., Copper, P., 1998. Oxygen and carbon isotopic composition of Silurian brachiopods: implications for coeval seawater and glaciations. *Geological Society of America Bulletin* 110, 1499–1512.
- Banner, J.L., Hanson, G.N., 1990. Calculation of simultaneous isotopic and trace element variations during water–rock interaction with applications to carbonate diagenesis. *Geochimica et Cosmochimica Acta* 54, 3123–3137.
- Bergström, S.M., Sweet, W.C., 1966. Conodonts from the Lexington Limestone (Middle Ordovician) of Kentucky and its lateral equivalents in Ohio and Indiana. *American Paleontology Bulletin* 50 (229), 271–441.
- Bergström, S.M., Carnes, J.B., Hall, J.C., Kurapkat, W., O’Neil, B.E., 1988. Conodont biostratigraphy of some Middle Ordovician stratotypes in the Southern and Central Appalachians. *New York State Museum Bulletin* 462, 20–32.
- Bergström, S.M., Huff, W.D., Kolata, D.R., Bauert, H., 1995. Nomenclature, stratigraphy, chemical fingerprinting, and aerial distribution of some Middle Ordovician K-bentonites in Baltoscandia. *GFF* 117, 1–13.
- Bergström, S.M., Saltzman, M.R., Ausich, W.I., 2003. Conodonts, graptolites, and $\delta^{13}\text{C}$ chemostratigraphy in the latest Ordovician (Gamachian, Hirnantian): a global review. *Abstracts with Programs-Geological Society of America* 35 (2), 14.
- Bergström, S.M., Huff, W.D., Saltzman, M.R., Kolata, D.R., Leslie, S.A., 2004. The greatest volcanic ash falls in the Phanerozoic: trans-Atlantic relations of the Ordovician Millbrig and Kinnekulle K-bentonites. *The Sedimentary Record* 2, 4–8.
- Brenchley, P.J., Marshall, J.D., Carden, G.F., Robertson, D.B., Long, D.F., Meidla, T., Hints, L., Anderson, T.F., 1994. Bathymetric and isotopic evidence for a short-lived late Ordovician glaciation in a greenhouse period. *Geology* 22, 295–298.
- Brenchley, P.J., Carden, G.F., Marshall, J.D., 1995. Environmental changes associated with the “first strike” of the Late Ordovician mass extinction. *Modern Geology* 20, 69–72.
- Brenchley, P.J., Carden, G.A., Hints, L., Kaljo, D., Marshall, J.D., Martma, T., Meidla, T., Nölvak, J., 2003. High-resolution stable isotope stratigraphy of Upper Ordovician sequences: constraints on the timing of bioevents and environmental changes associated with mass extinction and glaciation. *Geological Society of America Bulletin* 115 (1), 89–104.
- Broecker, W.S., Maier-Reimer, E., 1992. The influence of air and sea exchange on the carbon isotope distribution in the sea. *Global Biogeochemical Cycles* 6, 315–320.
- Buggisch, W., 2001. Carbon isotope analysis ($\delta^{13}\text{C}$) of Early to Middle Devonian carbonates from the Prague Syncline, the Carnic Alps, and the Montagne Noire (Czech Republic, Austria, France). *Earth Systems Processes Meeting, Programs with Abstracts*. Geological Society of America and Geological Society London, Edinburgh, Scotland, p. 70.
- Candelaria, M.P., Roux, B.P., 1997. Reservoir analysis of a horizontal-well completion in the Viola Limestone “chocolate brown zone”, Marietta Basin, Oklahoma. In: Johnson, K.S. (Ed.), *Simpson and Viola Groups in the Southern Midcontinent*, 1994 Symposium. Oklahoma Geological Survey Circular, vol. 99, pp. 183–193.
- Fezter, J.A., 1973. *Biostratigraphic Evaluation of some Middle Ordovician Bentonite Complexes in Eastern North America*. Unpublished M.S. Thesis. The Ohio State University, Columbus, OH.
- Finney, S.C., 1986. Graptolite biofacies and correlation of eustatic, subsidence, and tectonic events in the Middle to Upper Ordovician of North America. *Palaios* 1, 435–461.
- Finney, S.C., Berry, W.B., 1997. New perspectives on graptolite distributions and their use as indicators of platform margin dynamics. *Geology* 25 (10), 919–922.
- Finney, S.C., Berry, W.B., Cooper, J.D., Ripperdan, R.L., Sweet, W.C., Jacobson, S.R., Soufiane, A., Achab, A., Noble, P.J., 1999. Late Ordovician mass extinction: a new perspective from stratigraphic sections in central Nevada. *Geology* 27 (3), 215–218.
- Galvin, P.K., 1983. Deep to shallow carbonate ramp transition in Viola Limestone (Ordovician), southwest Arbuckle Mountains, Oklahoma. *American Association of Petroleum Geologists Bulletin* 63, 466–467.
- Gao, G., Dworkin, S.I., Land, L.S., Elmore, R.D., 1996. Geochemistry of Late Ordovician Viola Limestone, Oklahoma: implications for marine carbonate mineralogy and isotopic compositions. *Journal of Geology* 104, 359–367.
- Glumac, B., Walker, K.R., 1998. A Late Cambrian positive carbon-isotope excursion in the southern Appalachians: relation to biostratigraphy, sequence stratigraphy, environment of deposition, and diagenesis. *Journal of Sedimentary Research* 68, 1212–1222.
- Gruber, N., Keeling, C.D., Bacastow, R.B., Guenther, P.R., Lueker, T.J., Wahlen, M., Meijer, H.A.J., Mook, W.G., Stocker, T.F., 1999. Spatiotemporal patterns of carbon-13 in the global surface oceans and the oceanic Suess effect. *Global Biogeochemical Cycles* 13, 307–335.
- Hall, J.C., 1986. *Conodonts and Conodont Biostratigraphy of the Middle Ordovician in the Western Overthrust Region and Sequatchie Valley of the Southern Appalachians*. Unpublished PhD Dissertation. The Ohio State University, Columbus, OH.
- Hallock, P., 1988. The role of nutrient availability in bioerosion: consequences to carbonate buildups. *Palaeogeography, Palaeoclimatology, Palaeoecology* 63, 275–291.
- Hallock, P., Schlager, W., 1986. Nutrient excess and the demise of coral reefs and carbonate platforms. *Palaios* 1, 389–398.
- Hatch, J.R., Jacobson, S.R., Witzke, B.J., Risatti, J.B., Anders, D.E., Watney, W.L., Newell, K.D., Vuletich, A.K., 1987. Possible late Middle Ordovician carbon isotope excursion: evidence from Ordovician oils and hydrocarbon source rocks, Mid-Continent and East-Central United States. *American Association of Petroleum Geologists Bulletin* 71, 1342–1354.
- Haynes, J.T., 1992. Reinterpretation of Rocklandian (Upper Ordovician) K-bentonite stratigraphy in southwest Virginia, southeast West Virginia, and northeast Tennessee. *Virginia Division of Mineral Resources Publication* 126, 1–58.
- Haynes, J.T., 1994. The Ordovician Deicke and Millbrig K-bentonite beds of the Cincinnati Arch and the southern Valley

- and Ridge Province. Special Publication-Geological Society of America 290, 1–80.
- Herrmann, A.D., Haupt, B.J., Patzkowsky, M.E., Seidov, D., Slingerland, R.L., 2004. Response of Late Ordovician paleoceanography to changes in sea level, continental drift, and atmospheric $p\text{CO}_2$: potential causes for long-term cooling and glaciation. *Palaeogeography, Palaeoclimatology, Palaeoecology* 210, 385–401.
- Hladikova, J., Hladil, J., Kribek, B., 1997. Carbon and oxygen isotope records across Pridoli to Givetian stage boundaries in the Barrandian basin (Czech Republic). *Palaeogeography, Palaeoclimatology, Palaeoecology* 132, 2225–2241.
- Holland, S.M., Patzkowsky, M.E., 1996. Sequence stratigraphy and long-term paleoceanographic change in the Middle and Upper Ordovician of the eastern United States. Special Paper-Geological Society of America 306, 117–129.
- Holmden, C., Creaser, R.A., Muehlenbachs, K., Leslie, S.A., Bergström, S.M., 1998. Isotopic evidence for geochemical decoupling between ancient epeiric seas and bordering oceans: implications for secular curves. *Geology* 26 (6), 567–570.
- Huff, W.D., Bergström, S.M., Kolata, D.R., 1992. Gigantic Ordovician ash fall in North America and Europe: biological, tectomagmatic, and event-stratigraphic significance. *Geology* 20, 875–878.
- Jeppsson, L., 1990. An oceanic model for lithological and faunal changes tested on the Silurian record. *Journal of the Geological Society of London* 147, 663–674.
- Kaljo, D., Hints, L., Hints, O., Martma, T., Nõlvak, J., 2001. Carbon isotope stratigraphy in the latest Ordovician of Estonia. *Chemical Geology* 175, 49–59.
- Keith, C., 1989. Conodonts and Conodont Biostratigraphy of the Dolly Ridge Formation in Virginia and West Virginia. Unpublished B.S. Thesis, University of North Carolina, Wilmington, NC, 47 pp.
- Keith, C., Hall, J.C., 1989. Conodont Biostratigraphy of the Middle Ordovician carbonate to clastic transition in the Virginia–West Virginia border area. *Geological Society of America Abstracts with Programs* 21 (3) (23 p).
- Kolata, D.R., Huff, W.D., Bergström, S.M., 1996. Ordovician K-bentonites of Eastern North America. *Geological Society of America Special Paper*, vol. 313, pp. 1–84.
- Kolata, D.R., Huff, W.D., Bergström, S.M., 1998. Nature and regional significance of unconformities associated with the Middle Ordovician Hagan K-bentonite complex in the North American midcontinent. *Geological Society of America Bulletin* 6, 723–739.
- Kolata, D.R., Huff, W.D., Bergström, S.M., 2001. The Ordovician Sebree trough: an oceanic passage to the Midcontinent United States. *Geological Society of America Bulletin* 113 (8), 1067–1078.
- Kroopnick, P.M., 1985. The distribution of ^{13}C of ΣCO_2 in the world oceans. *Deep-sea Research* 32, 57–84.
- Kump, L.R., Arthur, M.A., Patzkowsky, M.E., Gibbs, M.T., Pinkus, D.S., Sheehan, P.M., 1999. A weathering hypothesis for glaciation at high atmospheric $p\text{CO}_2$ during the Late Ordovician. *Palaeogeography, Palaeoclimatology, Palaeoecology* 152, 173–187.
- Leslie, S.A., 1995. Upper Middle Ordovician Conodont Biofacies and Lithofacies Distribution Patterns in Eastern North America and Northwestern Europe: Evaluations Using Deicke, Millbrig, and Kinnekulle K-bentonite beds as time planes. Ph.D dissertation, The Ohio State University, Columbus, OH.
- Lin, H.-L., Wang, L.-W., Wang, C.-H., Gong, G.-C., 1999. Vertical distribution of $\delta^{13}\text{C}$ of dissolved inorganic carbon in the northeastern South China Sea. *Deep-Sea Research* 46, 757–775.
- Long, D.G.F., 1993. Oxygen and carbon isotopes and event stratigraphy near the Ordovician–Silurian boundary, Anticosti Island Quebec. *Palaeogeography, Palaeoclimatology, Palaeoecology* 104, 49–59.
- Ludvigson, G.A., Jacobson, S.R., Witzke, B.J., González, L.A., 1996. Carbonate component chemostratigraphy and depositional history of the Ordovician Decorah Formation, Upper Mississippi Valley. In: Witzke, B.J., Ludvigson, G.A., Day, J. (Eds.), *Paleozoic Sequence Stratigraphy: Views from the North American Craton*. Geological Society of America Special Paper, vol. 306, pp. 67–86.
- Ludvigson, G.A., Witzke, B.J., Schneider, C.L., Smith, E.A., Emerson, N.R., Carpenter, S.J., González, L.A., 2000. A profile of the Mid-Caradoc (Ordovician) carbon isotope excursion at the McGregor Quarry, Clayton County, Iowa. *Geological Society of Iowa Guidebook* 76, 25–31.
- Ludvigson, G.A., Witzke, B.J., Gonzalez, L.A., Carpenter, S.J., Schneider, C.L., Hasiuk, F., 2004. Late Ordovician (Turinian–Chatfieldian) carbon isotope excursions and their stratigraphic and paleoceanographic significance. *Palaeogeography, Palaeoclimatology, Palaeoecology* 210, 187–214.
- Magaritz, M., 1983. Carbon and oxygen isotope composition of recent and ancient coated grains. In: Peryt, T.M. (Ed.), *Coated Grains*. Springer, Berlin, pp. 27–37.
- Marshall, J.D., Brechley, P.J., Mason, P., Wolff, G.A., Astini, R.A., Hints, L., Meidla, T., 1997. Global carbon isotopic events associated with mass extinction and glaciation in the late Ordovician. *Palaeogeography, Palaeoclimatology, Palaeoecology* 132, 195–210.
- Mii, H., Grossman, E.L., Yancey, T.E., 1999. Carboniferous isotope stratigraphies of North America: implications for carboniferous paleoceanography and Mississippian glaciation. *Geological Society of America Bulletin* 111, 960–973.
- Mitchell, C.E., Adhya, S., Bergström, S.M., Joy, M.P., Delano, J.W., 2004. Discovery of the Ordovician Millbrig K-bentonite bed in the Trenton Group of New York State: implications for regional correlation and sequence stratigraphy in eastern North America. *Palaeogeography, Palaeoclimatology, Palaeoecology* 210, 331–346.
- Nielsen, A.T., 2004. Ordovician sea level changes: a Baltoscandian perspective. In: Webby, B.D., Paris, F., Droser, M.L., Percival, I.G. (Eds.), *The Great Ordovician Biodiversification Event*. Columbia Press, New York, pp. 84–93.
- Patterson, W.P., Walter, L.M., 1994. Depletion of ^{13}C in seawater ΣCO_2 on modern carbonate platforms: significance for the carbon isotopic record of carbonates. *Geology* 22, 885–888.
- Patzkowsky, M.E., Slupik, L.M., Arthur, M.A., Pancost, R.D., Freeman, K.H., 1997. Late Middle Ordovician environmental

- change and extinction: harbinger of the Late Ordovician or continuation of Cambrian patterns? *Geology* 25, 911–914.
- Perry Jr., W.J., 1972. The Trenton Group of Nittany Anticlinorium, eastern West Virginia. *West Virginia Geological and Economic Survey Circular* 13, 1–28.
- Pope, M.C., 2004. Cherty carbonate facies of the Montoya Group, southern New Mexico and western Texas and its regional correlatives: a record of Late Ordovician paleoceanography on southern Laurentia. *Palaeogeography, Palaeoclimatology, Palaeoecology* 210, 367–384.
- Pope, M.C., Read, J.F., 1997. High resolution stratigraphy of the Lexington Limestone (Late Middle Ordovician), Kentucky, USA: a cool-water carbonate-clastic ramp in a tectonically active foreland basin. In: James, N.P., Clarke, J. (Eds.), *Cool-Water Carbonates*. SEPM Special Publication, vol. 56, pp. 411–429.
- Pope, M.C., Read, J.F., 1998. Ordovician meter-scale cycles: implications for climate and eustatic fluctuations in the central Appalachians during a global greenhouse, non-glacial to glacial transition. *Palaeogeography, Palaeoclimatology, Palaeoecology* 138, 27–42.
- Pope, M.C., Steffen, J.B., 2003. Widespread, prolonged late Middle to Late Ordovician upwelling in North America: a proxy record of glaciation? *Geology* 31 (1), 63–66.
- Railsback, L.B., 1989. Ordovician Paleoceanography: Stable Isotope and C–S–Fe evidence from the Caradocian Trenton Group, Mohawk Valley, New York. Ph.D. dissertation, University of Illinois, Urbana-Champaign, Illinois.
- Railsback, L.B., Holland, S.M., Hunter, D.M., Jordan, E.M., Diaz, J.R., Crowe, D.E., 2003. Controls on geochemical expression of subaerial exposure in Ordovician limestones from the Nashville Dome, Tennessee, U.S.A. *Journal of Sedimentary Research* 73 (5), 790–805.
- Richardson, J.G., Bergström, S.M., 2003. Regional stratigraphic relations of the Trenton Limestone (Chatfieldian, Ordovician) in the eastern North American Midcontinent. *Northeastern Geology and Environmental Sciences* 18 (2), 93–115.
- Saltzman, M.R., 2001. Silurian $\delta^{13}\text{C}$ stratigraphy: a view from North America. *Geology* 29 (8), 671–674.
- Saltzman, M.R., 2002. Carbon isotope ($\delta^{13}\text{C}$) stratigraphy across the Silurian–Devonian transition in North America: evidence for a perturbation of the global carbon cycle. *Palaeogeography, Palaeoclimatology, Palaeoecology* 187, 83–100.
- Saltzman, M.R., Young, S.A., 2005. Long-lived glaciation in the Late Ordovician? Isotopic and sequence-stratigraphic evidence from western Laurentia. *Geology* 33, 109–112.
- Saltzman, M.R., Runnegar, B., Lohmann, K.C., 1998. Carbon isotope stratigraphy of Upper Cambrian (Steptoean Stage) sequences of the eastern Great Basin: record of a global oceanographic event. *Geological Society of America Bulletin* 110, 285–297.
- Saltzman, M.R., Brasier, M.D., Ripperdan, R.L., Ergaliev, G.K., Lohmann, K.C., Robinson, R.A., Chang, W.T., Peng, S., Runnegar, B., 2000. A global carbon isotope excursion (SPICE) during the Late Cambrian: relation to trilobite extinctions. *Palaeogeography, Palaeoclimatology, Palaeoecology* 162, 211–223.
- Saltzman, M.R., Bergström, S.M., Huff, W.D., Kolata, D.R., 2003. Conodont and graptolite biostratigraphy and the Ordovician (early Chatfieldian, Middle Caradocian) $\delta^{13}\text{C}$ excursion in North America and Baltoscandia: implications for the interpretations of the relations between the Millbrig and Kinnekulle K-bentonites. In: Albanesi, G.L., Beresi, M.S., Peralta, S.H. (Eds.), *Ordovician from the Andes*. Serie Correlacion Geologica, vol. 17. Instituto Superior De Correlacion Geologica (Insugeo), pp. 137–142.
- Saltzman, M.R., Runkel, A.C., Cowan, C.A., Runnegar, B., Stewart, M.C., Palmer, A.R., 2004. The upper Cambrian SPICE ($\delta^{13}\text{C}$) event and the Sauk II–Sauk III regression: New evidence from Laurentian basins in Utah, Iowa, and Newfoundland. *Journal of Sedimentary Research* 74, 366–377.
- Scotese, C.R., McKerrow, W.S., 1991. Ordovician plate tectonic reconstructions. In: Barnes, C.R., Williams, S.H. (Eds.), *Advances in Ordovician Geology*. Geological Survey of Canada Paper, vol. 90-9, pp. 271–282.
- Sigman, D.M., Boyle, E.A., 2000. Glacial/interglacial variations in atmospheric carbon dioxide. *Nature* 407, 859–869.
- Simo, J.A., Emerson, N.R., Byers, C.W., Ludvigson, G.A., 2003. Anatomy of an embayment in an Ordovician epicritic sea, Upper Mississippi Valley, USA. *Geology* 31 (6), 545–548.
- Sweet, W.C., 1979. Conodonts and conodont biostratigraphy of post-Tyrone Ordovician rocks of the Cincinnati region. *United States Geological Survey Professional Paper* 1066-G, 1–26.
- Sweet, W.C., 1983. Conodont biostratigraphy of Fite Formation and Viola Group. *Oklahoma Geological Survey Bulletin* 132, 23–36.
- Sweet, W.C., 1984a. Graphic correlation of upper Middle and Upper Ordovician rocks, North American Midcontinent Province, USA. In: Bruton, D.L. (Ed.), *Aspects of the Ordovician System*, *Palaeontological Contributions from the University of Oslo* 295. Universitetsforlaget, Oslo, pp. 23–36.
- Sweet, W.C., 1984b. The Conodonta: morphology, taxonomy, paleoecology, and evolutionary history of a long-extinct animal phylum. *Oxford Monographs on Geology and Geophysics* 10, 152–156.
- Sweet, W.C., Bergström, S.M., 1984. Conodont provinces and biofacies of the late Ordovician. *Geological Society of America Special Paper*, vol. 196, pp. 69–88.
- Sweet, W.C., Harper Jr., H., Zlatkin, D., 1974. The American Upper Ordovician Standard: XIX. A Middle and Upper Ordovician Standard for the Eastern Cincinnati region. *Ohio Journal of Science* 74, 47–54.
- Votaw, R.B., 1971. Conodont Biostratigraphy of the Black River Group (Middle Ordovician) and Equivalent Rocks of the Eastern Midcontinent, North America. Unpublished Ph.D. dissertation, The Ohio State University, Columbus, OH.
- Wilde, P., 1991. Oceanography in the Ordovician. In: Barnes, C.R., Williams, S.H. (Eds.), *Advances in Ordovician Geology*. Geological Survey of Canada Paper, vol. 90-9, pp. 283–298.
- Witzke, B.J., 1990. Palaeoclimatic constraints for Paleozoic paleolatitudes of Laurentia and Euramerica. In: McKerrow, W.S., Scotese, C.R. (Eds.), *Palaeogeography and Biogeography*. Geological Society Memoir, vol. 12, pp. 57–73.